

UNCLASSIFIED

AD **259 682**

*Reproduced
by the*

**ARMED SERVICES TECHNICAL INFORMATION AGENCY
ARLINGTON HALL STATION
ARLINGTON 12, VIRGINIA**



UNCLASSIFIED

NOTICE: When government or other drawings, specifications or other data are used for any purpose other than in connection with a definitely related government procurement operation, the U. S. Government thereby incurs no responsibility, nor any obligation whatsoever; and the fact that the Government may have formulated, furnished, or in any way supplied the said drawings, specifications, or other data is not to be regarded by implication or otherwise as in any manner licensing the holder or any other person or corporation, or conveying any rights or permission to manufacture, use or sell any patented invention that may in any way be related thereto.

NASA TN D-872

259682



CATALOGED BY ASIIA
AS AD NO. —

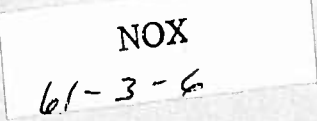
TECHNICAL NOTE

D-872

EFFECT OF IMPINGEMENT ANGLE ON DROP-SIZE DISTRIBUTION
AND SPRAY PATTERN OF TWO IMPINGING WATER JETS

By Marcus F. Heidmann and Hampton H. Foster

Lewis Research Center
Cleveland, Ohio



NATIONAL AERONAUTICS AND SPACE ADMINISTRATION
WASHINGTON

July 1961

NATIONAL AERONAUTICS AND SPACE ADMINISTRATION

TECHNICAL NOTE D-872

EFFECT OF IMPINGEMENT ANGLE ON DROP-SIZE DISTRIBUTION

AND SPRAY PATTERN OF TWO IMPINGING WATER JETS

By Marcus F. Heidmann and Hampton H. Foster

SUMMARY

E-1301

The spray formed by two 0.089-inch-diameter water jets was investigated for impingement angles of 10° to 90° and jet velocities of 30 to 74 feet per second. Photographs of the overall spray pattern formed in quiescent air show greater dispersion and reduced liquid sheet length for larger impingement angles. Jet-velocity effects were less pronounced.

Drop-size distributions were obtained with the spray formed in a 100-foot-per-second airstream. Drop counts were made from shadowgraph photographs using an electronic particle analyzer. All distributions showed bimodal characteristics with number-median diameters of about 200 and 600 microns for the two modes. The most significant effect of impingement angle and jet velocity on the distributions was a change in the relative number of drops in each mode and the geometric mean deviation of the larger drop-size mode. An increase in impingement angle produced an increase in the number of small drops and a decrease in the deviation of the larger drop-size mode. This effect was most pronounced at low jet velocities. Mass-median diameters and relative mass in the two modes were determined from the basic number-size distributions, and the effect of angle and velocity was evaluated. At all test conditions the larger drop-size mode contained the majority of the mass.

Overall volume-number mean and mass-median drop diameters were obtained for each condition. Both parameters increased with a decrease in impingement angle, the largest increase occurring at low jet velocities.

INTRODUCTION

The angle of impingement between two liquid jets is a frequently varied parameter in liquid atomizers for rocket-engine combustors. Such angle changes affect combustor efficiency and stability in a manner not wholly explained on the basis of present knowledge of liquid sprays. It

is the purpose of this study to evaluate the characteristic properties of the liquid spray for various impingement angles. Specifically, properties of the drop-size distribution have been investigated for water sprays in an airstream at room temperature.

The study was made with two 0.089-inch-diameter impinging water jets using impingement angles of 10°, 30°, 40°, 60°, and 90° over a range of jet velocities from 30 to 74 feet per second. Drop-size data were obtained from 1:1 shadowgraph photographs taken 8 inches downstream of the point of jet impingement. These photographs were taken in a duct at 100-foot-per-second air velocity. Drop images were counted with a particle analyzer with electron-beam scanning and digital output.

Drop-size distributions were found to be bimodal in all cases. Characteristic properties of each mode and of the combined modes were evaluated. The effect of impingement angle on these properties at various jet velocities is presented.

Photographs of the spray formed in quiescent air were also taken to study overall spray-pattern changes with impingement angle and jet velocity.

APPARATUS AND PROCEDURE

Impinging-Jet Atomizers

The design of the impinging-jet atomizers is shown in figure 1. Five separate atomizers with jet diameters of 0.089 inch and impingement angles of 10°, 30°, 40°, 60°, and 90° were used. The spacing between the centerline of the tube exit was kept at a constant value of 0.35 inch for each atomizer. The jet diameter and spacing approximate those used in combustor studies reported in references 1 to 3 and spray studies reported in references 4 and 5.

A gas-pressurized water-flow system with a 40-gallon tank was used. Flow rates were indicated by a rotating-vane flowmeter and electronic counter. Flow rates were established to produce jet velocities of 30, 44, 60, and 74 feet per second. These velocities were calculated from flow continuity but were experimentally verified in reference 4 to be the jet velocity without air resistance.

Spray-Pattern Photographs

Shadowgraph photographs using diffused light were taken to characterize the overall spray pattern formed in quiescent air. An area of

approximately 8 by 10 inches was photographed. Photographs were taken for each of the five impingement angles and four jet-velocity conditions.

Drop Photographs

Shadowgraph photographs using parallel light and a 1:1 magnification were taken to obtain drop-size distribution data. The photographs were taken with the spray in an air duct. The duct and optical system are shown in figure 2. The duct is basically a 12- by 4-inch section; however, an extension on the 4-inch width was needed to eliminate splashing along the optical path. Photographs were taken with the optical path normal to the plane of the essentially two-dimensional spray pattern formed by impinging jets. The centerline of the optical path intercepted the spray axis 8 inches downstream of the point of jet impingement for all photographs. An air velocity of 100 feet per second and atmospheric pressure were used in all cases. Five photographs were taken at random times for each test condition. Test conditions consisted of the five impingement angles at four jet velocities.

Drop-Size Analysis

An electronic particle analyzer described in reference 6 was used to obtain drop counts used in this study. With this analyzer, drop counts can be made directly from either positive or negative transparencies. An area up to 20 by 20 millimeters may be scanned at one time. Particles in the size range of 200 to 6400 microns can be counted. This range is covered in 10 steps that vary by a ratio of $\sqrt{2}$. All particles larger than a preselected size are counted, and particles in a particular size range are obtained by a difference in counts. The count is digitally displayed.

The principle of operation is as follows. The photograph is scanned by an electronic flying spot system. The transmitted light falls on a photomultiplier tube producing voltage signals related to the opacity of the film. Each time the scanning spot is intercepted by a particle, an impulse is produced. This signal is compared with that produced by the previous scan. If the particle did not intercept the previous scan, a pulse is passed to the counter; otherwise, this pulse is suppressed. In this manner a single count is produced for each particle. An ultrasonic delay line is used to compare successive scans.

Sizing is accomplished by a system that allows only the pulses greater than a preselected length to pass to the counter. Thus, particles are sized by their maximum dimensions in the line-scanning direction. The image area of the film is covered by 100 line scans in 1/10 second. Variations are minimized by recording the impulses from ten

complete scans for each sizing condition. Recycling is possible every 7 seconds.

For monitoring purposes the film area under examination is displayed on a 12-inch cathode-ray tube. Each particle that is counted is shown by a bright marker tag on the display tube.

Sizing accuracy is adjustable. Master photographs containing known numbers of various size drops are used for the adjustment.

RESULTS AND DISCUSSION

Spray Pattern in Quiescent Air

The effect of impingement angle and jet velocity on the overall spray pattern is shown in the photographs of figure 3. Waves of drop resulting from intermittent disintegration appear in all the patterns. These fluctuations were studied and reported in reference 7. Figure 3 shows that, for a 90° impingement angle, mass is circumferentially distributed around the point of impingement with the highest mass concentration along the spray axis. This is in agreement with reference 5, where properties of a 90° -impingement-angle spray were studied. The most pronounced effect of a decrease in impingement angle is the increase in mass concentration along the spray axis. At an angle of 10° , mass is confined to a dispersion angle of about 20° . This increase in mass concentration is accompanied by an increase in the length of unbroken liquid surface in the spray. At a 90° impingement angle the region of unbroken liquid sheet is not readily evident but extended only a short distance from the point of impingement, certainly less than an inch. At a 10° angle it extended about 9 inches from the point of impingement.

Figure 4 shows the approximate effect of impingement angle on the length of liquid sheet. The approximate effect on the limit of drop dispersion is also shown. The effect of jet velocity on these values appears to be small and is not shown in figure 4, although a small increase in dispersion and decrease in liquid sheet length were observed with an increase in velocity. These are the properties of a free spray. The properties in an airstream were not evaluated because of the inability to obtain such photographs within the confines of the air duct.

Drop-Size Distribution in Airstream

Experimental results. - An example of the shadowgraph photographs used in the airstream to obtain drop-size data is shown in figure 5. Atomization was shown to be incomplete at the 8-inch distance for a 10° impingement angle, and drop-sizing was not attempted for this condition.

Ligament formation also appears to exist for the 30° impingement angle. A distribution of drops is present, however, and counts obtained for these drops were used in analyzing the results.

The drop counts obtained with the electronic analyser are listed in table I. Drop diameters smaller than 200 microns, although present, were not sized because they were beyond the resolution limit of the photograph-analyzer system.

The number-size distributions provided by these counts are shown in figure 6. The log of the number of drops in a drop-size group as a function of the log of the drop diameter is shown for each test condition. The drop-size groups are those obtained directly from the particle analyzer. These groups are all similar in that the ratio of the maximum to the minimum size in each group is equal to $\sqrt{2}$. A typical logarithmic-normal distribution evaluated on the basis of such groupings and plotted as in figure 6 would produce a smooth symmetrical distribution curve with a single maximum point. In many of the curves of figure 6, however, two inflection points are evident. This indicates that the distributions may be bimodal, that is, composed of two separated distributions. In the analysis of the data it was assumed that all distributions were the summation of two logarithmic-normal distributions. Such an analysis was used because physical processes of atomization would be expected to be more fundamentally related to the properties of each mode than to any overall property of the distribution.

Previous evidence of bimodal distributions. - Bimodal properties for impinging-jet sprays of this type were obtained in a study reported to the Fifth International Congress on High-Speed Photography. In this study a 30,000-drop count was obtained for the free spray of a 90°-impingement-angle injector. These results are shown in figure 7. Both the number-size and mass-size distributions are shown. A bimodal characteristic is distinctly evident in both distributions. Also shown in figure 7 are two logarithmic-normal distributions that add to give a good fit to the experimental data.

In reference 4 Ingebo studied heptane sprays produced by impinging-jet injectors. The Nukiyama-Tanasawa analysis was used to examine drop distribution. A reexamination of these data showed that bimodal characteristics were evident in most of the distributions. Figure 8 shows an example of these data. The drop counts have been normalized to correspond to that obtained from the particle analyzer. The drop counts in reference 4 were scaled from photomicrographs for relatively small increments in drop size. Drop counts are small for such groupings and cause random variations in the distribution curve. Many of the distributions show these irregularities, which complicate the bimodal evaluation. The existence of at least two major modes, however, appears conclusive.

Bimodal characteristics of liquid sprays produced by other types of atomizers have also been previously reported and treated analytically (refs. 8 and 9). These investigators postulated that multimodal distributions exist because several factors that produce distinct distributions contribute to the complete atomization in a liquid spray.

Selection of modes. - The two distribution curves used to give a good fit to the experimental data in figure 6 cannot be considered precise. It must be realized that for each mode the magnitude, geometric mean deviation, and median drop size can be varied. These parameters can be varied significantly while maintaining a good fit to the data. Even with such limitations, the bimodal analysis may prove profitable in providing some insight into fundamental properties of distributions from impinging-jet sprays.

It was found through repeated curve-fitting that the geometric mean deviation of approximately 1.5 for the first mode (the mode with the smaller drops) was obtained. In the final analysis, the value was fixed at 1.5 and the other parameters were adjusted to give the best fit. In making the fit the smaller drop-size counts were generally weighted more heavily than the count for larger drops. In the larger drop groupings, with 1 to 10 drops, a larger deviation from the true distribution could be expected. Although it is difficult to justify the particular parameters selected, some of the properties that will be presented are not significantly affected by the goodness of the fit.

Median drop sizes. - The median drop size of each mode in the distributions is shown in figure 9. The number-median drop size and the mass-median drop size are shown as a function of impingement angle for each jet velocity. The number-median sizes are the medians of the curves in figure 6. No significant effect of impingement angle or jet velocity is evident on the number median of the first mode. Although variations exist, no consistent trend beyond experimental scatter can be justified. The number-median diameter of the first mode has an average value of 180 to 190 microns.

A more consistent effect of impingement angle and jet velocity is evident in the number median of the second mode. The median appears to have a minimum value in the region of 60° to 70° for each jet velocity. The median generally decreases with an increase in jet velocity; however, the smallest value was obtained with a jet velocity of 60 feet per second. Values obtained at the 30° impingement angle are the least reliable because of the incomplete atomization occurring at this condition. The trends developed in this region are not considered significant.

The mass-median drop sizes were obtained analytically from the number-median distributions. From reference 10 the relation between the mass-median and number-median sizes for a logarithmical-normal distribution may be expressed as

$$\frac{\text{Mass median}}{\text{Number median}} = e^{3(\log \sigma_g)^2}$$

where σ_g is the geometric mean deviation of the distribution. The deviations of the first mode were constant at 1.5. Deviations for the second mode are shown in figure 10. The deviation is shown to increase with a decrease in impingement angle. The deviation also increased with a decrease in jet velocities; however, an inversion occurred in this effect at angles greater than about 80°.

Mass-median sizes were calculated using these deviations. These mass medians are shown in figure 9. Mass medians of the first mode again show no significant trend, since they are directly proportional to the number median. An average value of 300 to 310 microns is shown for the mass-median diameter. The mass-median diameter of the second mode shows the most pronounced effect of implngement angle. Values range from about 900 microns at the 90° angle to 2000 microns at smaller angles. Low jet velocities show the largest increase in size with a decrease in angle. Although low jet velocities generally show the largest median sizes, this trend appears to approach an inversion in the region of 90°.

The relation between the first- and second-mode median sizes is shown in figure 11. The ratio of the second- to the first-mode median sizes is shown as a function of impingement angle. The number-median size ratio does not show a large change with impingement angle. The number median of the second mode is about 3 times that of the first mode. The trends shown may not be significant because of the accuracy of curve-fitting.

The ratio of mass medians increases with a decrease in impingement angle, the largest effect occurring at low jet velocities. Values of 3 to 8 are shown. Low jet velocities generally show the largest ratio; however, an inversion in this effect is developing at large impingement angles.

This inversion noted in the second-mode characteristics may be the result of operating conditcns. All sprays were tested in an environmental velocity of 100 feet per second so that aerodynamic forces contributed to the atomization process. This force should increase as jet velocity decreases. The force would also be large on any liquid in motion lateral to the normal spray axis. Such lateral flow increases as impingement angle increases. The combination of changes in dispersion and aerodynamic forces could cause the observed inversion in the second-mode characteristics.

Number and mass ratios. - The number of drops and liquid mass represented by the distribution modes of figure 6 were also evaluated. The absolute values are not significant; however, the relative magnitudes are a characteristic parameter. Figure 12 shows the ratio of the number of drops in the second mode to that in the first mode. At an impingement angle of 90° there are about 5 to 6 times as many drops in the mode with the small median size as in that for the large median size. As impingement angle decreases, the number of drops in each mode become more nearly equal. It differs by about 25 percent at an angle of 40° . The values shown for 30° may not be reliable because of the sampling difficulties incurred at this condition. As a generality, the ratio of the number of drops in the second mode to that in the first mode is inversely proportional to the impingement angle.

The ratio of masses of the second mode to that of the first is shown as a function of impingement angle in figure 13. The second mode always contains the most mass; however, the ratio varies by an order of magnitude for the range of impingement angle studied. The ratio again varies inversely with impingement angle. At an angle of 90° the second mode contains about 4 times the mass of the first mode.

Overall Spray Characteristics

A mean drop size is frequently determined for a distribution of drops for the purpose of describing a spray with a single quantitative value. Two such sizes were evaluated from the entire distribution defined by the two modes. These sizes were the volume-number mean and the mass median. The volume-number mean is the drop size of a uniform spray having the same volume and number of drops as the complete distribution. The mass median is the drop size for which the masses in drops larger and smaller than the median size are equal.

Volume-number mean. - The volume-number mean size is shown in figure 14. At an impingement angle of 90° the mean diameter is about 380 microns with no significant effect of jet velocity. The mean diameter increased with a decrease in angle, the effect being largest for low jet velocities. Mean diameters are shown to vary inversely to about the 0.6 power of impingement at 74 feet per second and to the 0.9 power at 30 feet per second.

The values of volume-number mean diameter are lower than those obtained by direct integration of the experimental data. The lower value results from the extrapolation of the first-mode distribution in the small size region. Reporting this lower value is partially justified because drops smaller than 200 microns were not measured in the counting technique used even though smaller drops were known to exist in the distribution. The values shown for 90° are in agreement with those obtained

E-1301

with heptane by Ingebo (ref. 4) when adjusted for the difference in surface tension.

Mass median. - A mass-median drop diameter is also frequently used to describe a particular spray. The variation in mass-median diameter with impingement angle is shown in figure 15. The overall mass-median diameters are very nearly equal to that for the second mode (fig. 9), particularly at low impingement angles. At 90° the mass median is nearly constant at about 780 microns, although a slightly higher value is shown for a jet velocity of 74 feet per second. The relatively constant diameter with changes in jet velocity for a 90° impingement angle was also observed in reference 5. The empirical correlation derived by Ingebo (ref. 4) also shows that increasing jet velocity increases jet-impact forces but decreases aerodynamic forces and thus may account for the relatively constant mean diameter. At smaller impingement angles mean diameter increases more rapidly with a decrease in jet velocities. An approximate description of the observed trends is that drop diameter varies inversely with the 0.4 power of impingement angle at 74 feet per second to about inverse proportionality at 30 feet per second.

Concluding Remarks

Test conditions used in this study were selected to give engineering data on the effect of impingement angle on rocket combustor atomizers. The jet diameter and the range of angles and jet velocities compare with those commonly employed in rocket combustors. The airstream velocity, gas density, and flow Reynolds number also approximate the combustion-gas conditions existing in the region of spray formation in many rocket combustors. However, the effect of liquid properties and the environment changes caused by combustion on these results are needed for a direct application to combustors. Even with these limitations the observed trends in the spray pattern and overall spray characteristics would be expected to persist.

The bimodal characteristic observed in the distribution curves suggests a relation to fundamental processes involved in liquid atomization. The selection of test conditions, however, was not suitable for evaluating such a relation. Aerodynamic drag forces in particular were not controlled. Aerodynamic and liquid jet parameters must be varied independently. Such data are needed to determine how bimodal properties are related to the force and momentum processes of atomization.

SUMMARY OF RESULTS

A pair of 0.089-inch-diameter impinging jets of water was investigated over a range of impingement angles and jet velocities in a 100-foot-per-second air duct. The following results were obtained:

1. Photographs of a spray in free air showed disintegration to occur closer to the point of jet impingement and angular dispersion to increase as impingement angle increased.
2. Drop-size distributions obtained with an electronic particle analyzer from shadowgraph photographs showed bimodal distribution characteristics at all test conditions.
3. The number-median diameter of the two modes in the distribution were in the region of 200 microns for one mode and 600 microns for the other. The ratio of these medians was equal to about 3, with no significant effect of impingement angle or jet velocity.
4. The mass-median drop diameter remained relatively constant at 300 microns for one mode and ranged from about 900 to 2000 microns for the other mode. In the large size mode, the median size increased with a decrease in impingement angle; the largest effect occurred at low jet velocities. The ratio of mass-median diameters showed a similar variation.
5. With a geometric mean deviation of the mode with the smaller drop equal to 1.5, the deviation of the mode with larger drops varied between 1.45 and 1.9. The lowest values of deviation were observed for a 90° impingement angle. Deviation increased with a decrease in angle, the low jet velocities giving the largest increase.
6. The ratio of the number of drops in the large drop-size mode to the small size mode varied from about 1/6 at 90° to about 3/4 at 40°. The effect of jet velocity was not large. The mass in the large size mode, however, was 4 times as large as that in the small mode at 90° and increased to 40 to 75 times as large at low angles. The largest ratios occurred at low jet velocities.
7. The overall volume-number mean drop diameter increased from about 380 microns at a 90° impingement angle to 700 to 1000 microns at a 30° angle, with low jet velocities giving the largest effect.
8. The overall mass-median drop diameter increased from about 800 microns at a 90° impingement angle to 1200 to 2500 microns at a 30° angle. The largest effect occurred at low jet velocities.

E-1301

REFERENCES

1. Heidman, M. F.: Propellant Vaporization as a Criterion for Rocket-Engine Design; Experimental Effect of Fuel Temperature on Liquid-Oxygen - Heptane Performance. NACA RM E57E03, 1957.
2. Clark, Bruce J., Hersch, Martin, and Priem, Richard J.: Propellant Vaporization as a Criterion for Rocket-Engine Design; Experimental Performance, Vaporization, and Heat-Transfer Rates with Various Propellant Combinations. NASA MEMO 12-29-58E, 1959.
3. Heidmann, Marcus F.: Propellant Vaporization as a Criterion for Rocket-Engine Design; Experimental Effect of Chamber Diameter on Liquid Oxygen - Heptane Performance. NASA TN D-65, 1959.
4. Ingebo, Robert D.: Drop-Size Distribution for Impinging-Jet Breakup in Airstreams Simulating the Velocity Conditions in Rocket Combustors. NACA TN 4222, 1958.
5. Foster, Hampton H., and Heidmann, Marcus F.: Spatial Characteristics of Water Spray Formed by Two Impinging Jets at Several Jet Velocities in Quiescent Air. NASA TN D-301, 1960.
6. Dell, H. A., Hobbs, D. S., and Richards, M. S.: An Automatic Particle Counter and Sizer. Philips Tech. Rev., vol. 21, no. 9, Aug. 1960, pp. 253-267.
7. Heidmann, Marcus F., Priem, Richard J., and Humphrey, Jack C.: A Study of Sprays Formed by Two Impinging Jets. NACA TN 3835, 1957.
8. Kottler, F.: The Distribution of Particle Sizes. Jour. Franklin Inst., vol. 250, no. 4, Oct. 1950, pp. 339-356.
9. Dallavalle, J. M., Orr, C., Jr., and Blocker, H. G.: Fitting Bimodal Partical Size Distribution Curves. Ind. and Eng. Chem., vol. 43, no. 6, June 1951, pp. 1377-1380.
10. Bevans, Rowland S.: Mathematical Expressions for Drop Size Distributions in Sprays. Conf. on Fuel Sprays, Univ. Mich., Mar. 30-31, 1949.

TABLE I. - DROP COUNTS FOR VARIOUS TEST CONDITIONS
OBTAINED WITH PARTICLE ANALYZER

Drop-size range, microns	Number of drops				Drop-size range, microns	Number of drops				
	Impingement angle, deg					Impingement angle, deg				
	90	60	40	30		90	60	40	30	
Jet velocity, 74 ft/sec					Jet velocity, 44 ft/sec					
200-280	1058	687	408	129	200-280	720	393	209	165	
280-400	446	362	267	99	280-400	352	233	130	103	
400-560	250	250	213	96	400-560	219	152	123	93	
560-800	208	174	164	104	560-800	139	93	104	84	
800-1120	75	70	105	60	800-1120	59	56	73	59	
1120-1600	31	18	40	44	1120-1600	10	21	35	51	
1600-2240	7	4	13	58	1600-2240	1	8	17	43	
2240-3200	4	---	5	31	2240-3200	---	2	9	26	
3200-4525	---	---	1	20	3200-4525	---	---	2	10	
4525-6400	---	---	---	---	4525-6400	---	---	---	---	
Total	2109	1565	1216	641	Total	1500	958	702	634	
Jet velocity, 60 ft/sec					Jet velocity, 30 ft/sec					
200-280	589	660	259	145	200-280	639	531	185	291	
280-400	365	336	191	77	280-400	276	243	110	169	
400-560	204	250	161	81	400-560	165	192	99	113	
560-800	128	162	137	94	560-800	126	137	104	83	
800-1120	38	90	87	71	800-1120	47	90	75	76	
1120-1600	14	22	41	58	1120-1600	7	35	49	56	
1600-2240	2	7	13	37	1600-2240	---	13	14	24	
2240-3200	---	2	9	31	2240-3200	---	3	4	23	
3200-4525	---	---	---	17	3200-4525	---	---	---	5	
4525-6400	---	---	---	---	4525-6400	---	---	---	---	
Total	1340	1529	898	611	Total	1260	1244	640	840	

E-1501

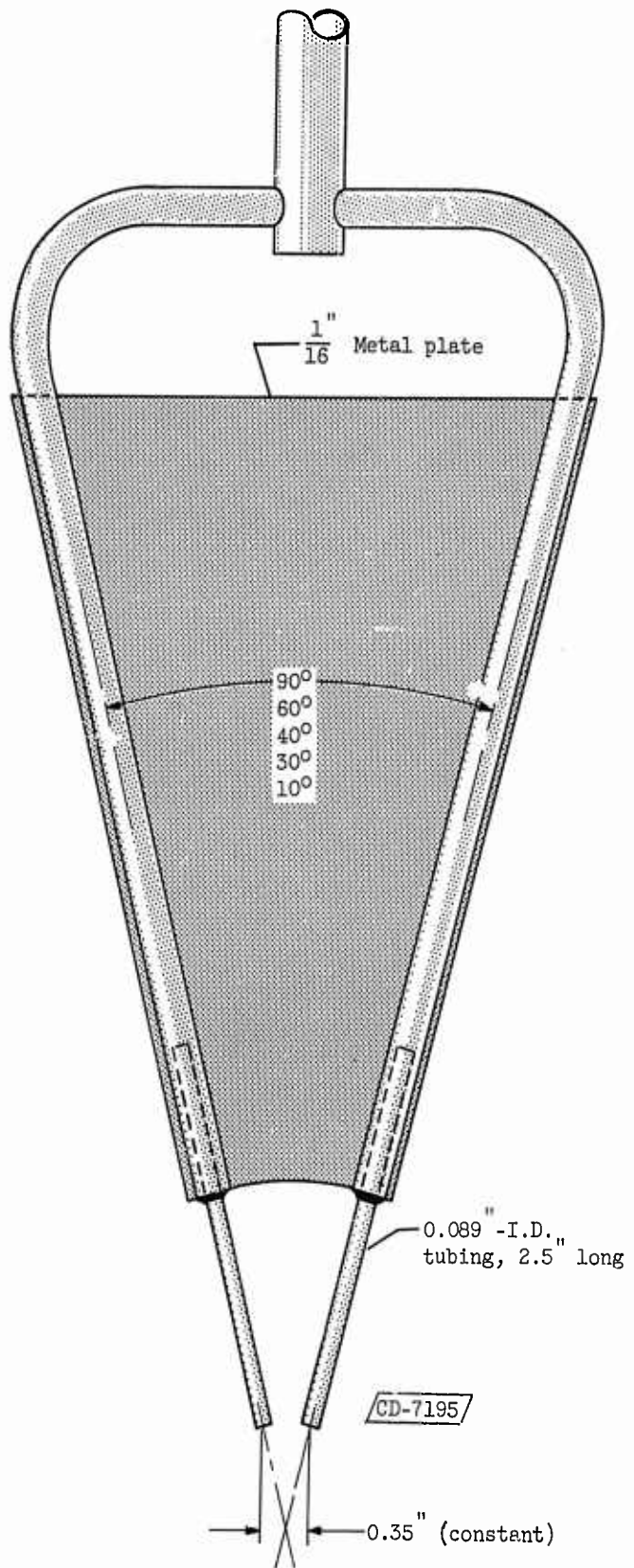


Figure 1. - Impinging-jet injector.

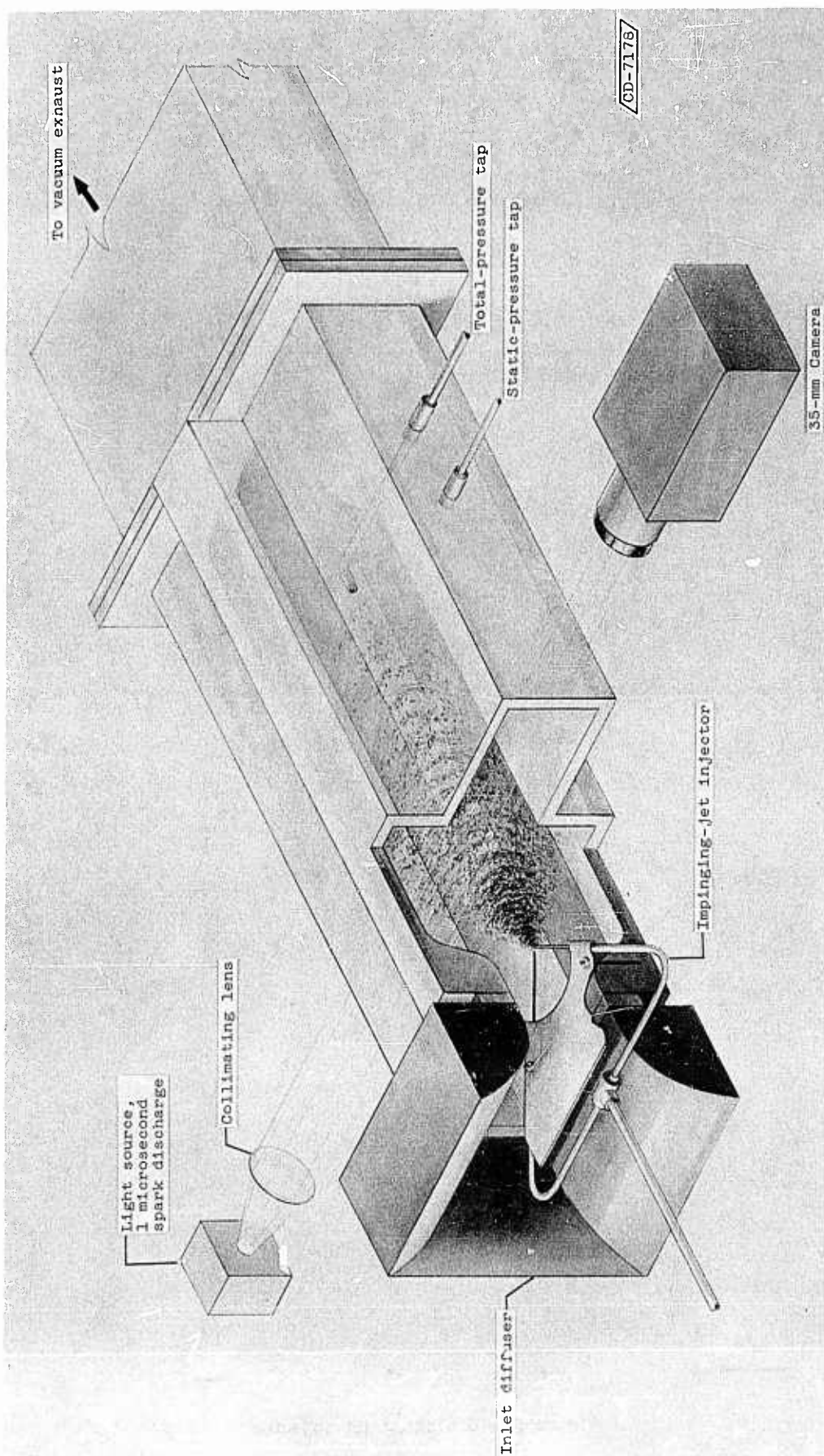


Figure 2. - Experimental apparatus used for drop photographs in air duct.

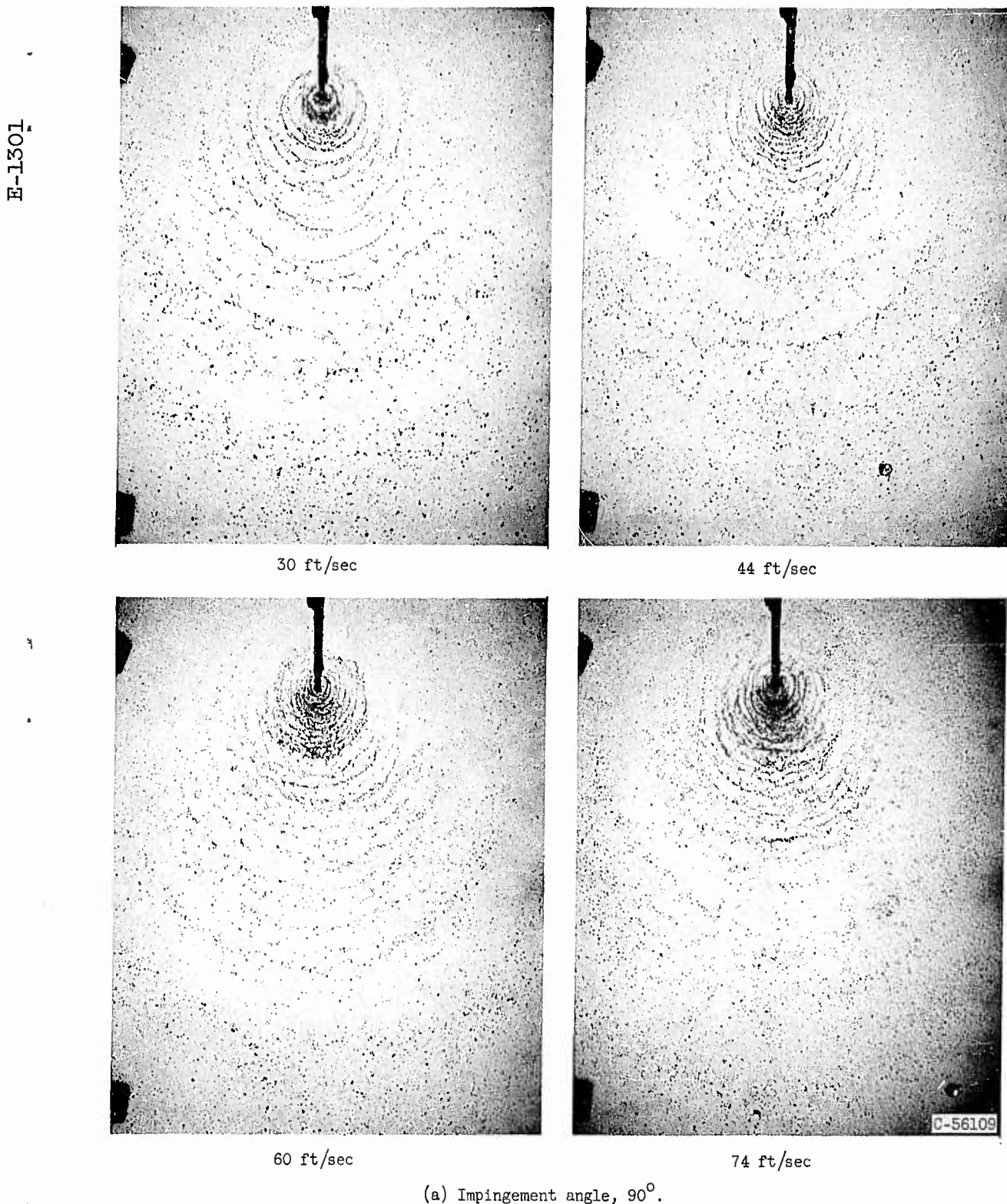


Figure 3. - Spray pattern of impinging jets in free air.

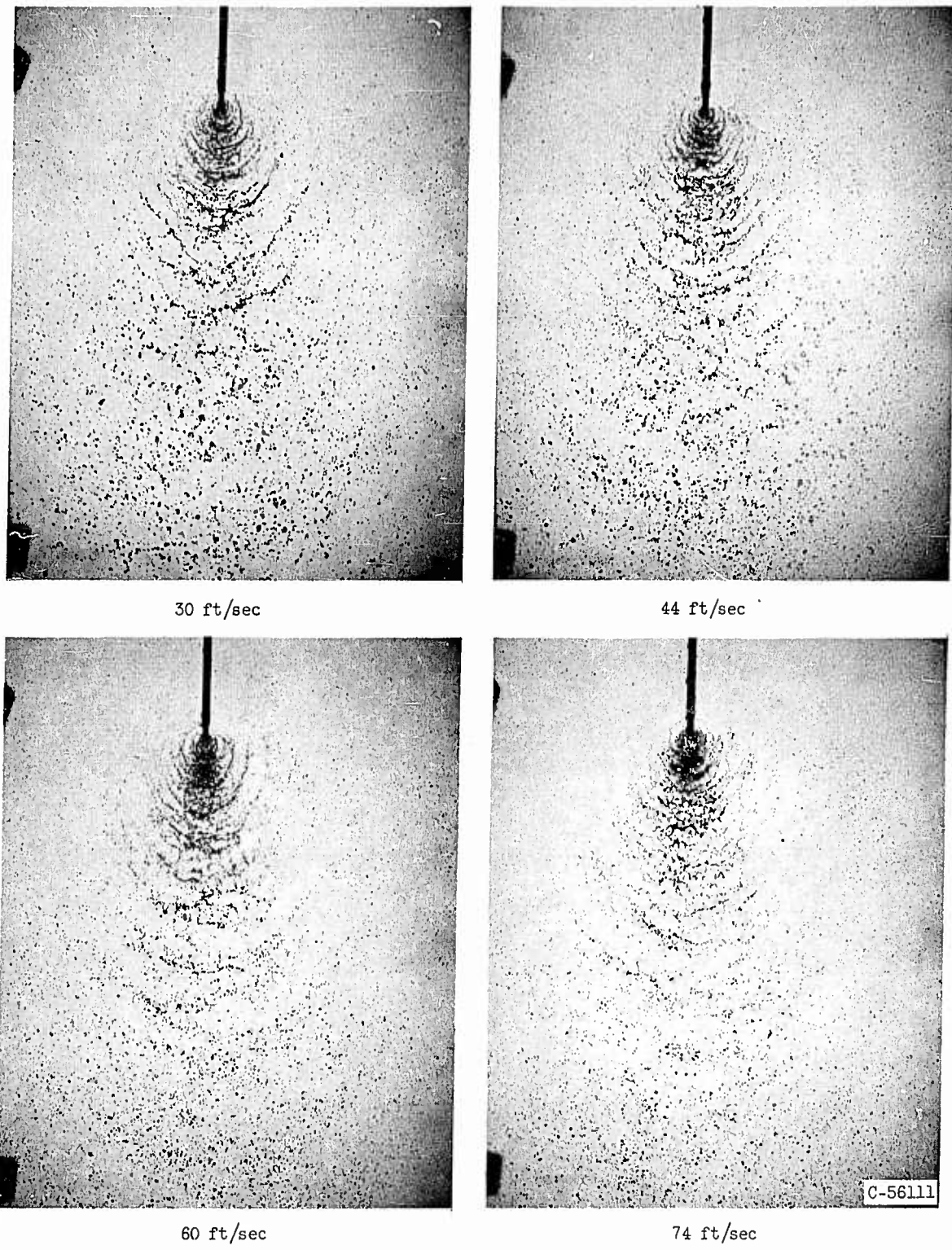
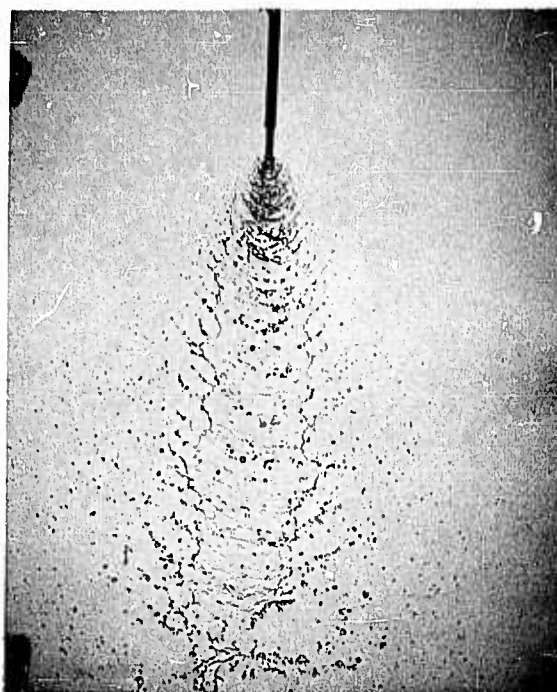
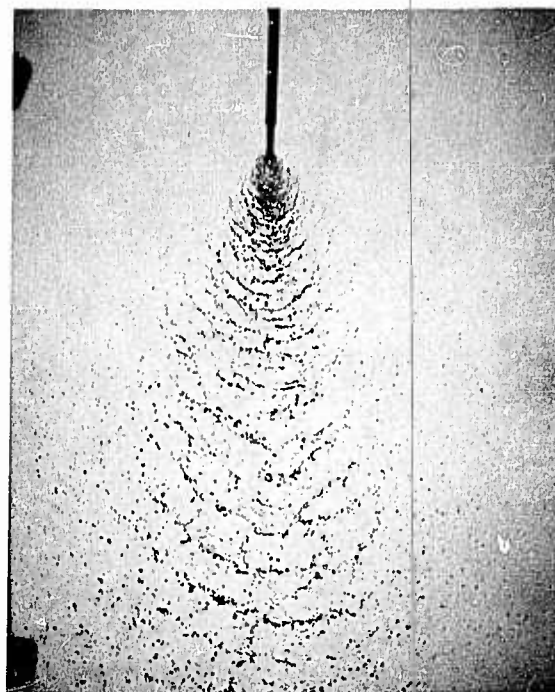
(b) Impingement angle, 60° .

Figure 3. - Continued. Spray pattern of impinging jets in free air.

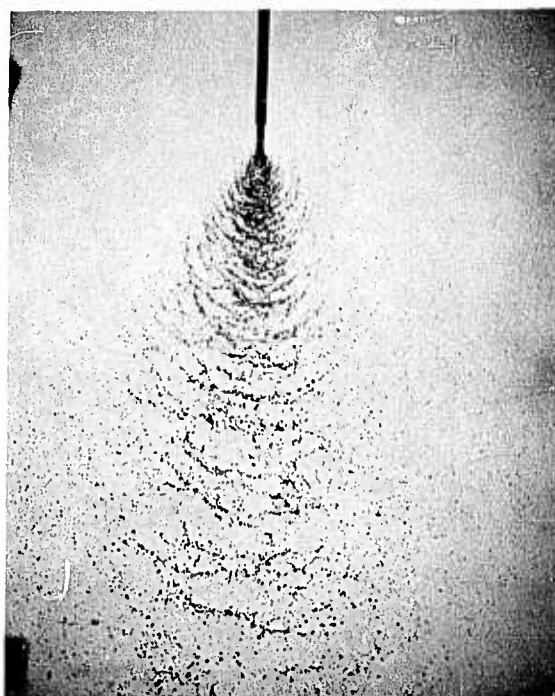
E-1301



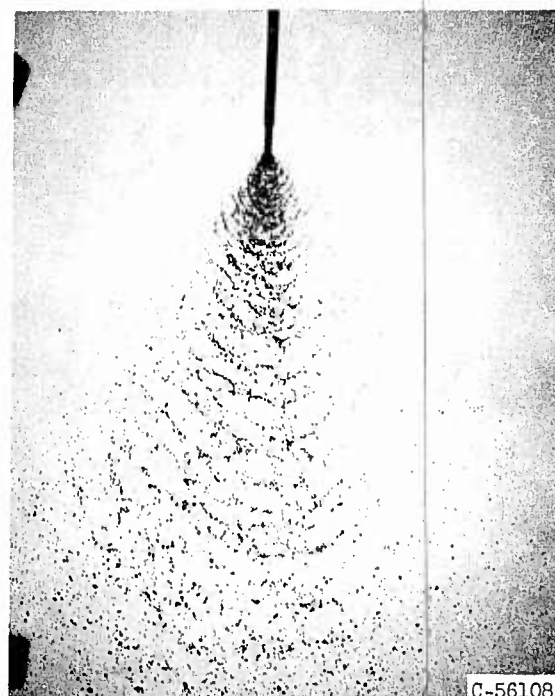
30 ft/sec



44 ft/sec



60 ft/sec



74 ft/sec

C-56108

(c) Impingement angle, 40° .

Figure 3. - Continued. Spray pattern of impinging jets in free air.

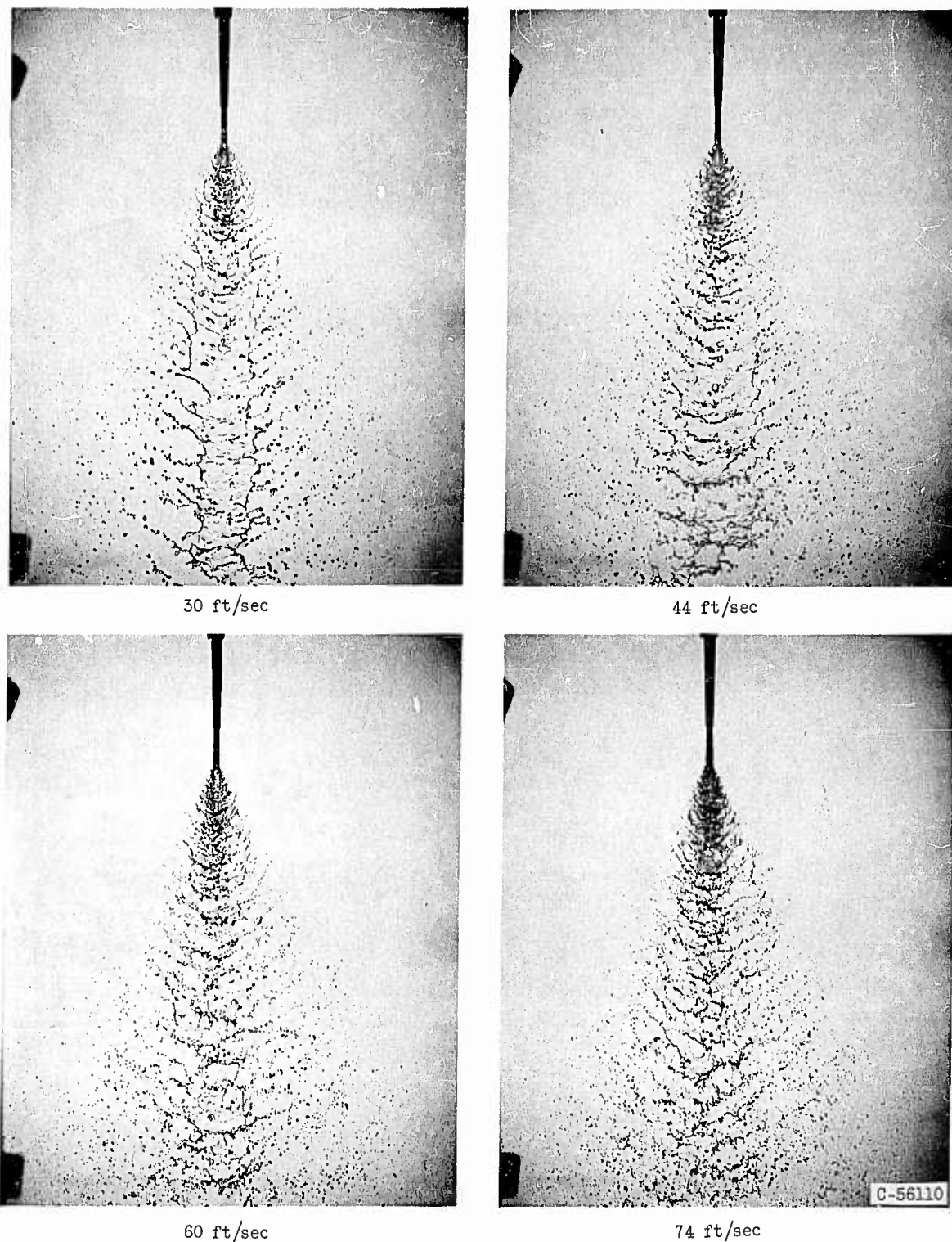
(d) Impingement angle, 30° .

Figure 3. - Continued. Spray pattern of impinging jets in free air.

E-1501

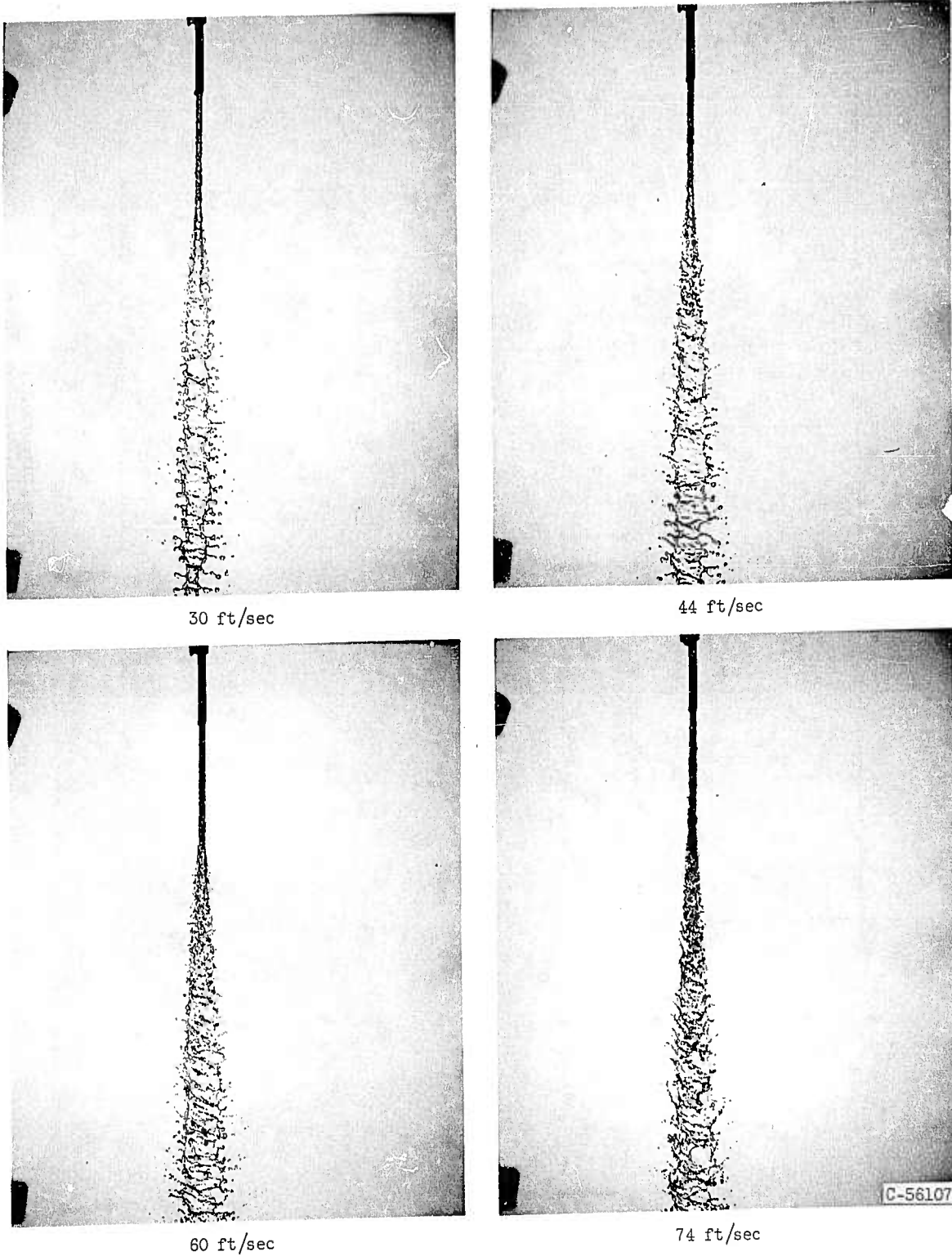
(e) Impingement angle, 10° .

Figure 3. - Concluded. Spray pattern of impinging jets in free air.

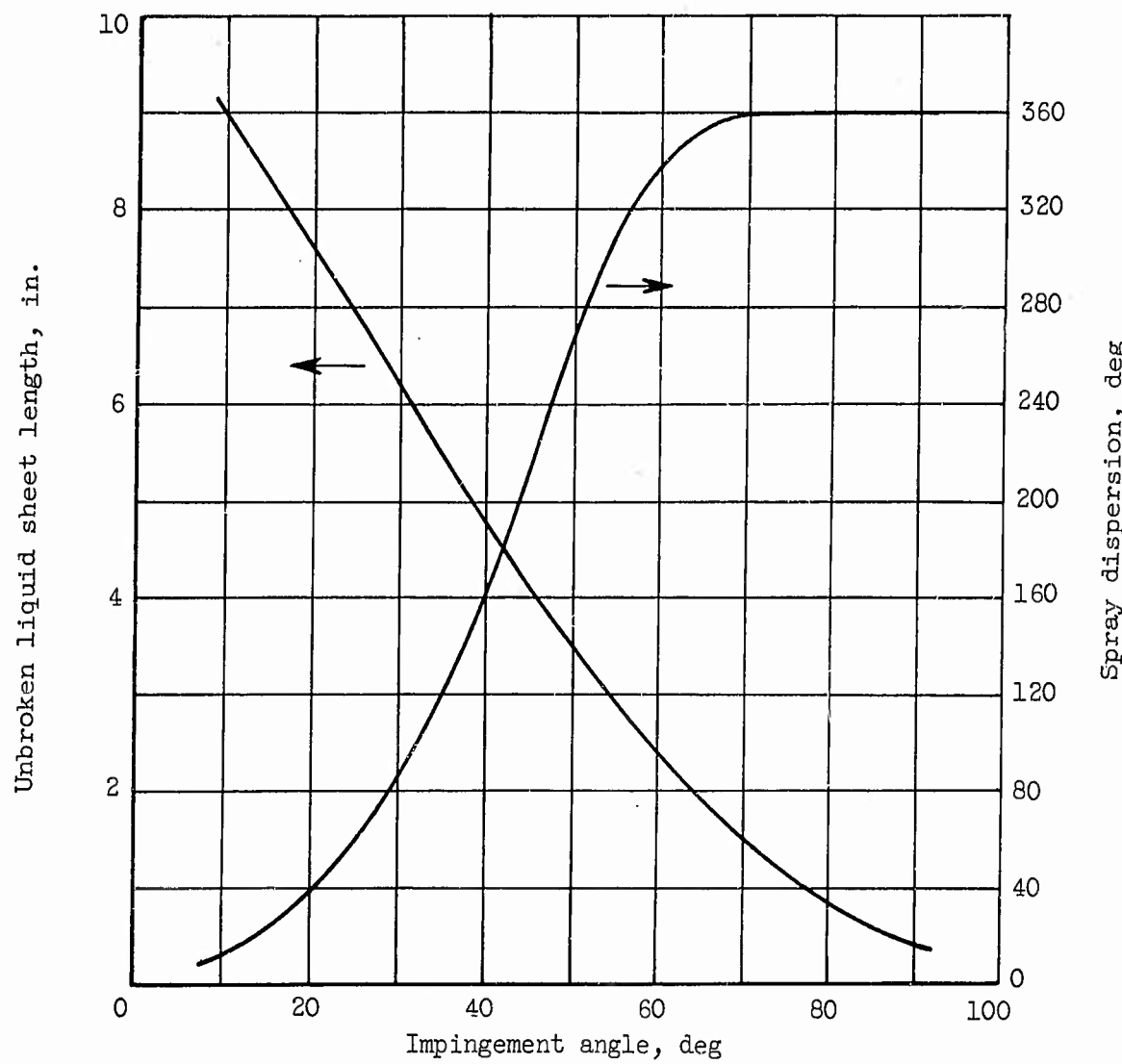


Figure 4. - Approximate values of liquid sheet length and spray dispersion.

E-1301

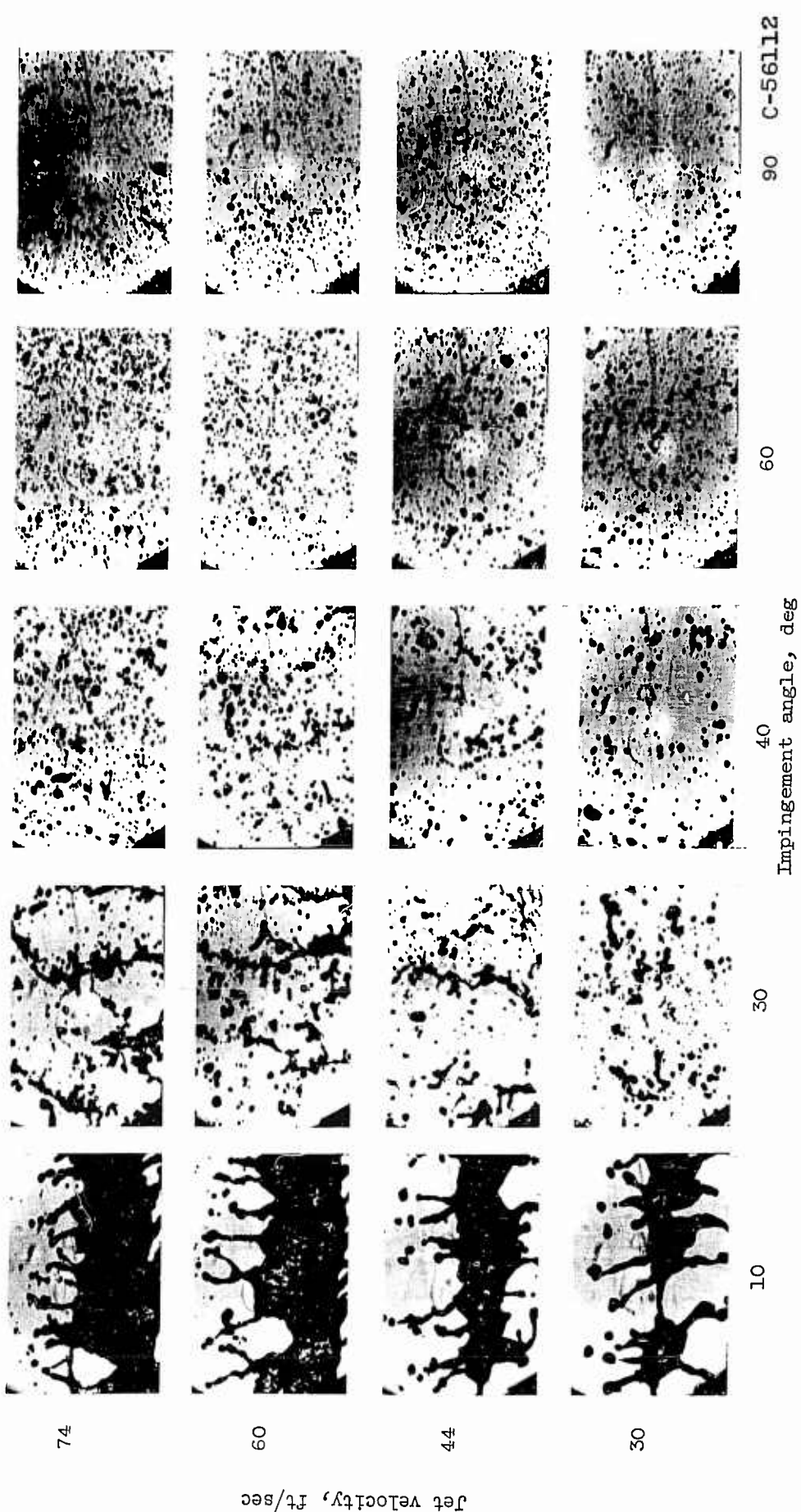


Figure 5. - Typical shadowgraph photographs of drop distributions 8 inches downstream of impingement point.

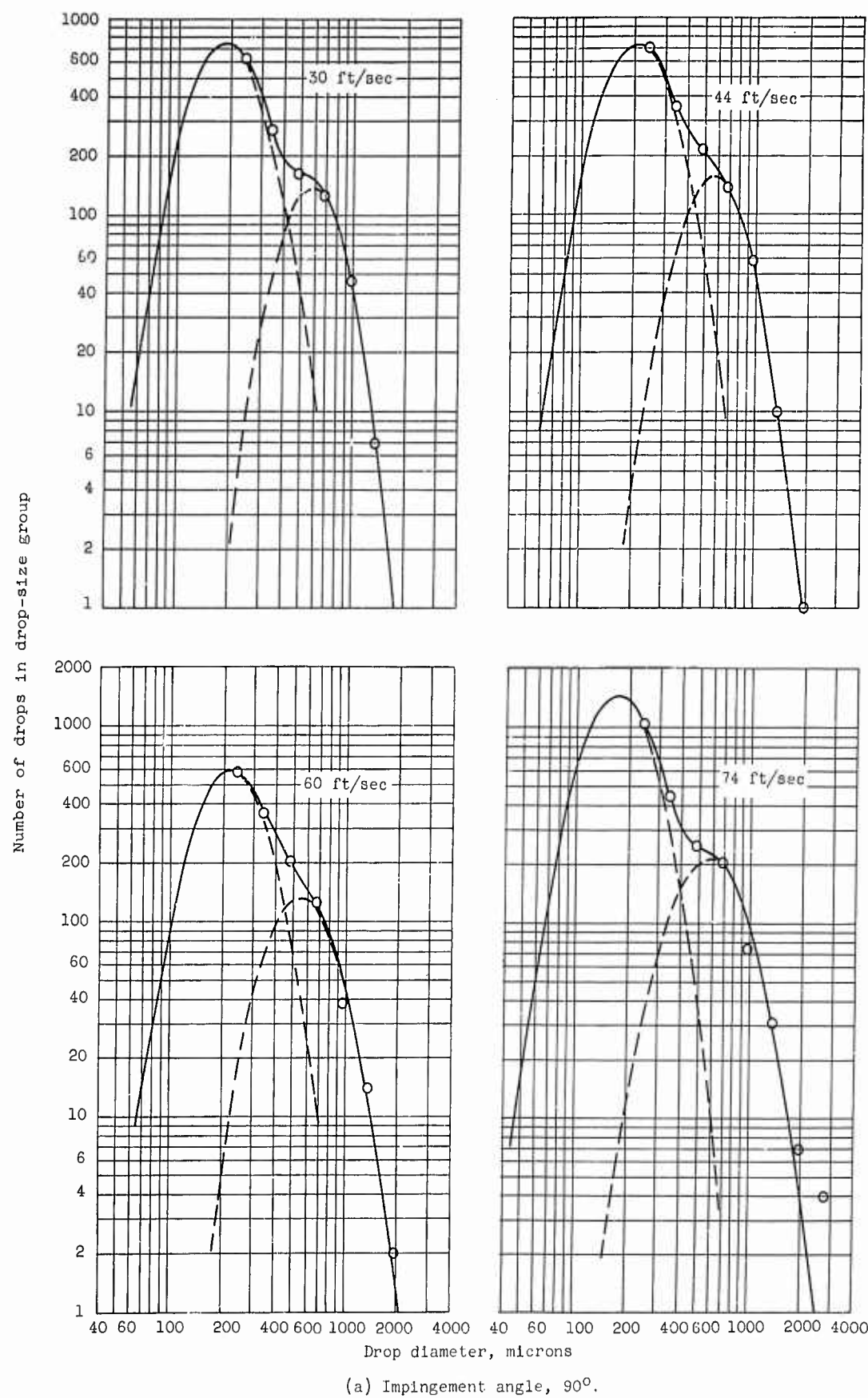
(a) Impingement angle, 90° .

Figure 6. - Number-size distribution for various jet velocities.

E-1301.

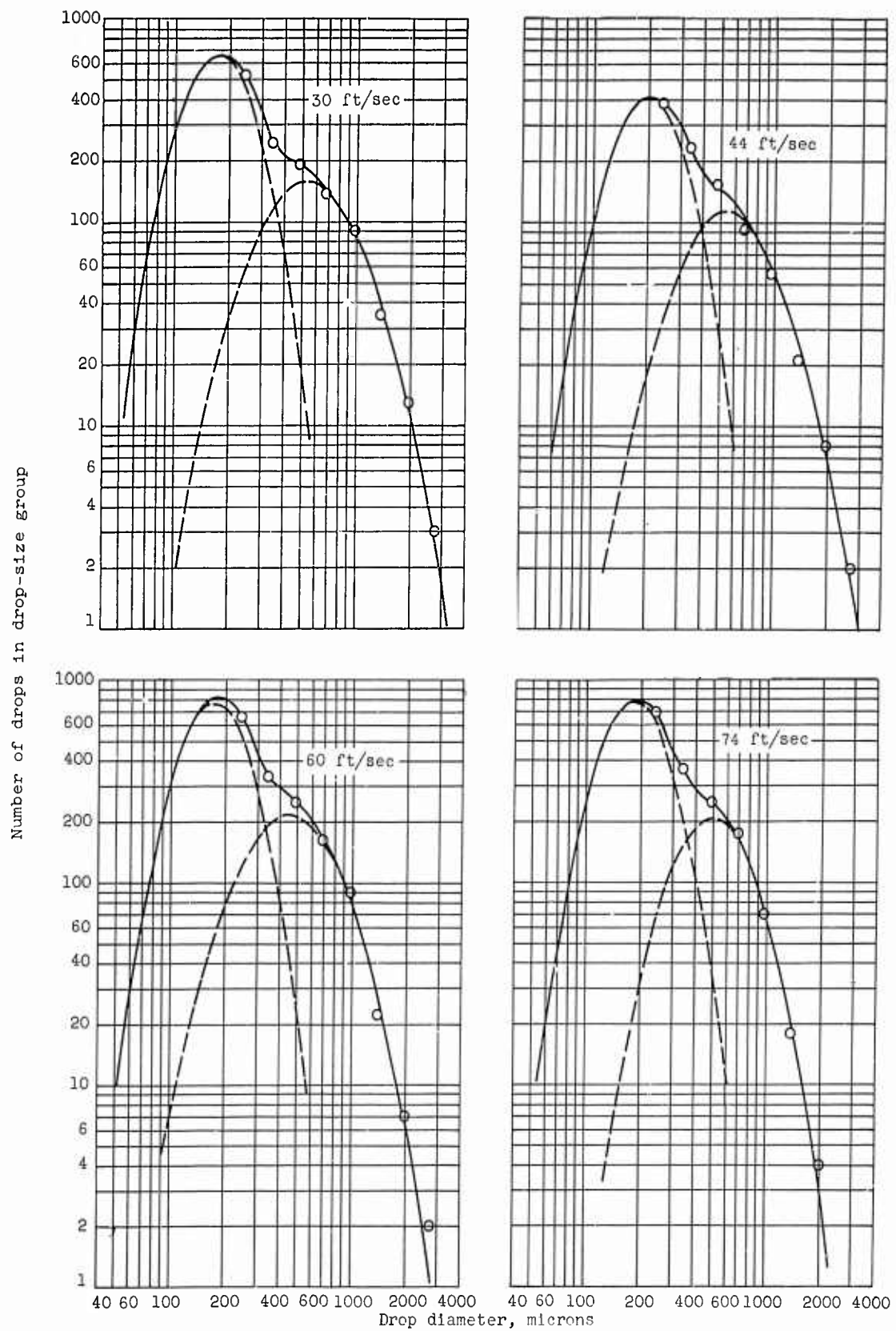
(b) Impingement angle, 60° .

Figure 6. - Continued. Number-size distribution for various jet velocities.

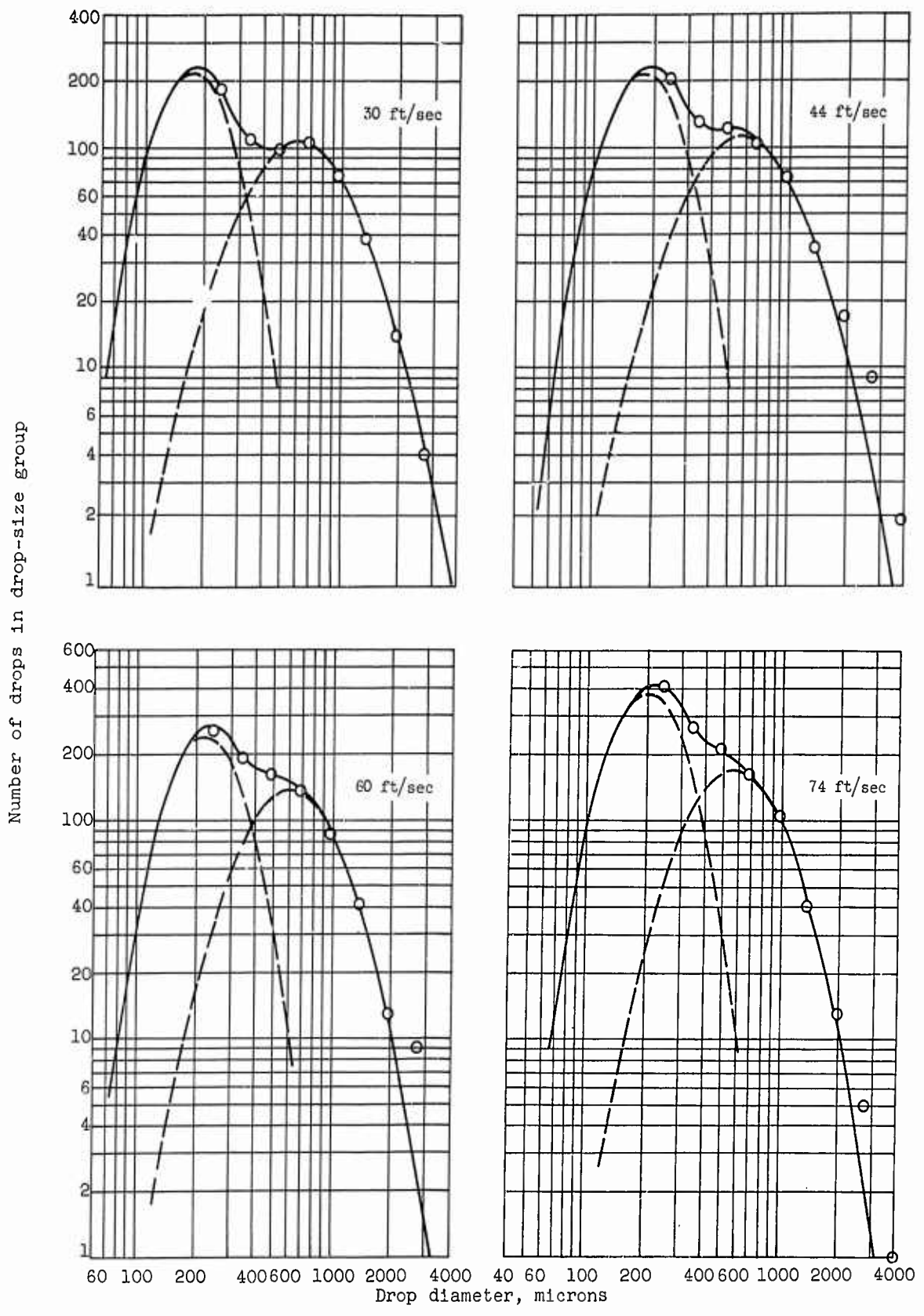
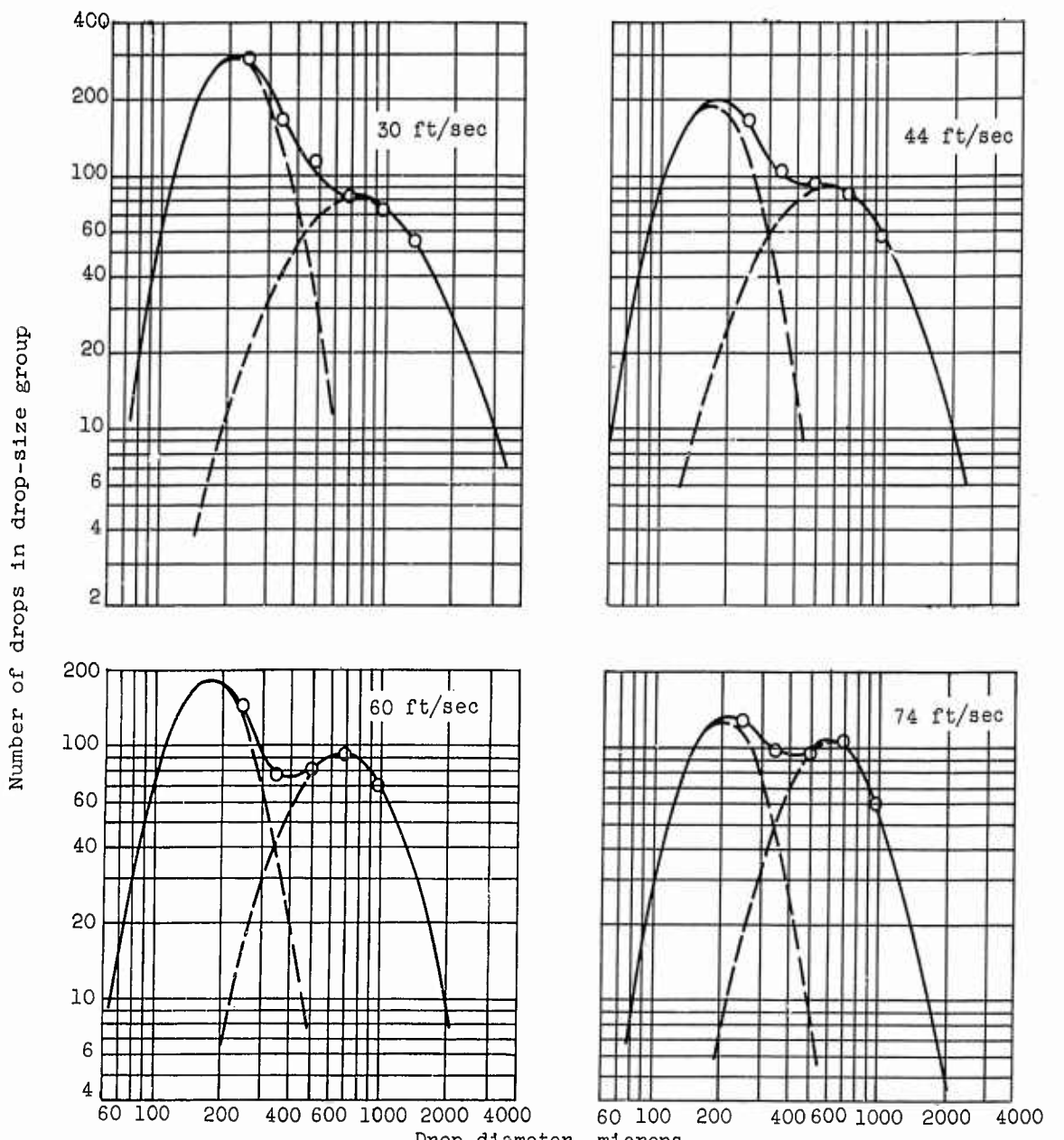
(c) Impingement angle, 40° .

Figure 6. - Continued. Number-size distribution for various jet velocities.

E-1301



(d) Impingement angle, 30°.

Figure 6. - Concluded. Number-size distribution for various jet velocities.

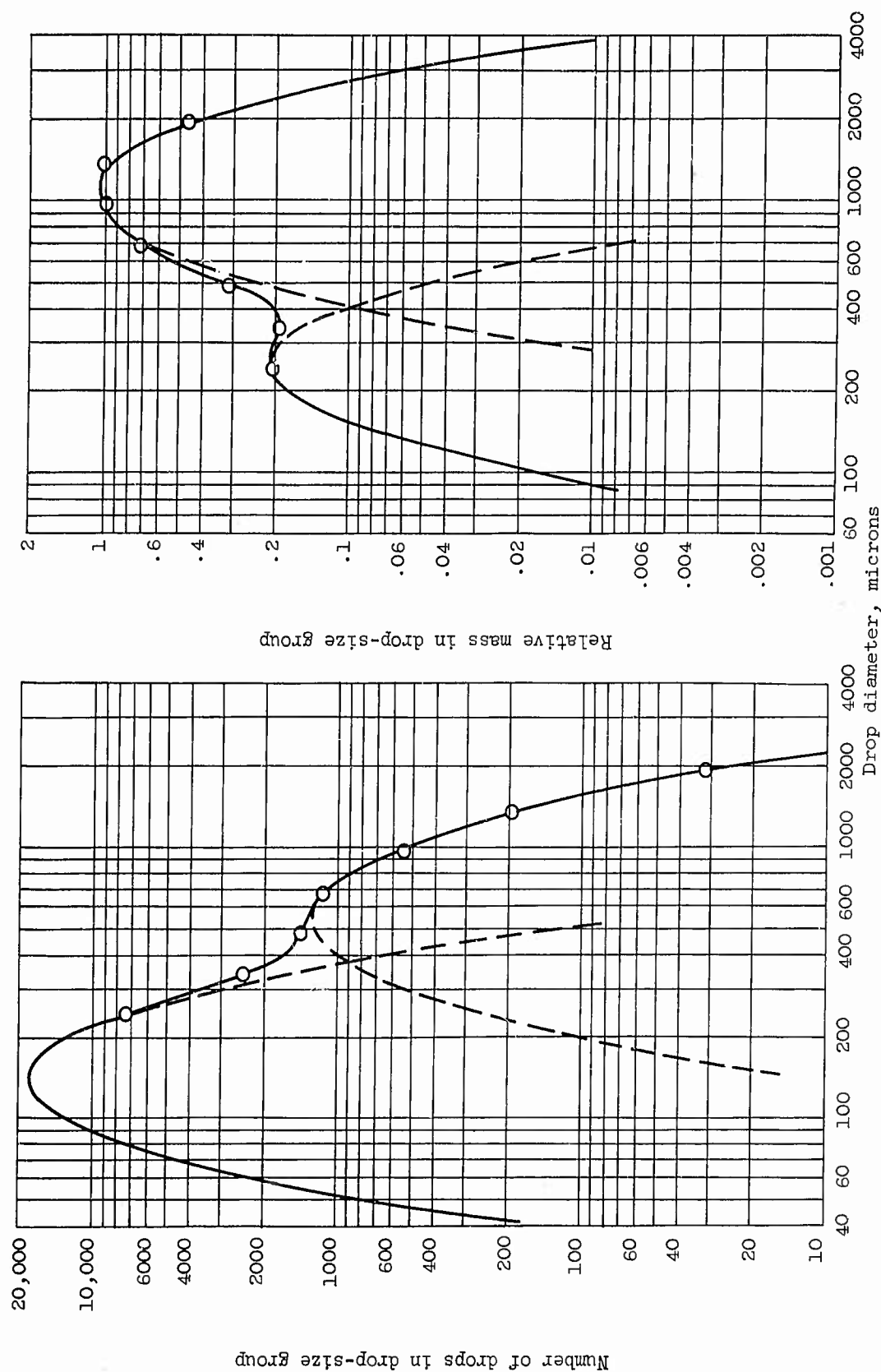


Figure 7. - Bimodal characteristics of number-size and mass-size distributions obtained in 30,000-drop sample of impinging-jet spray.

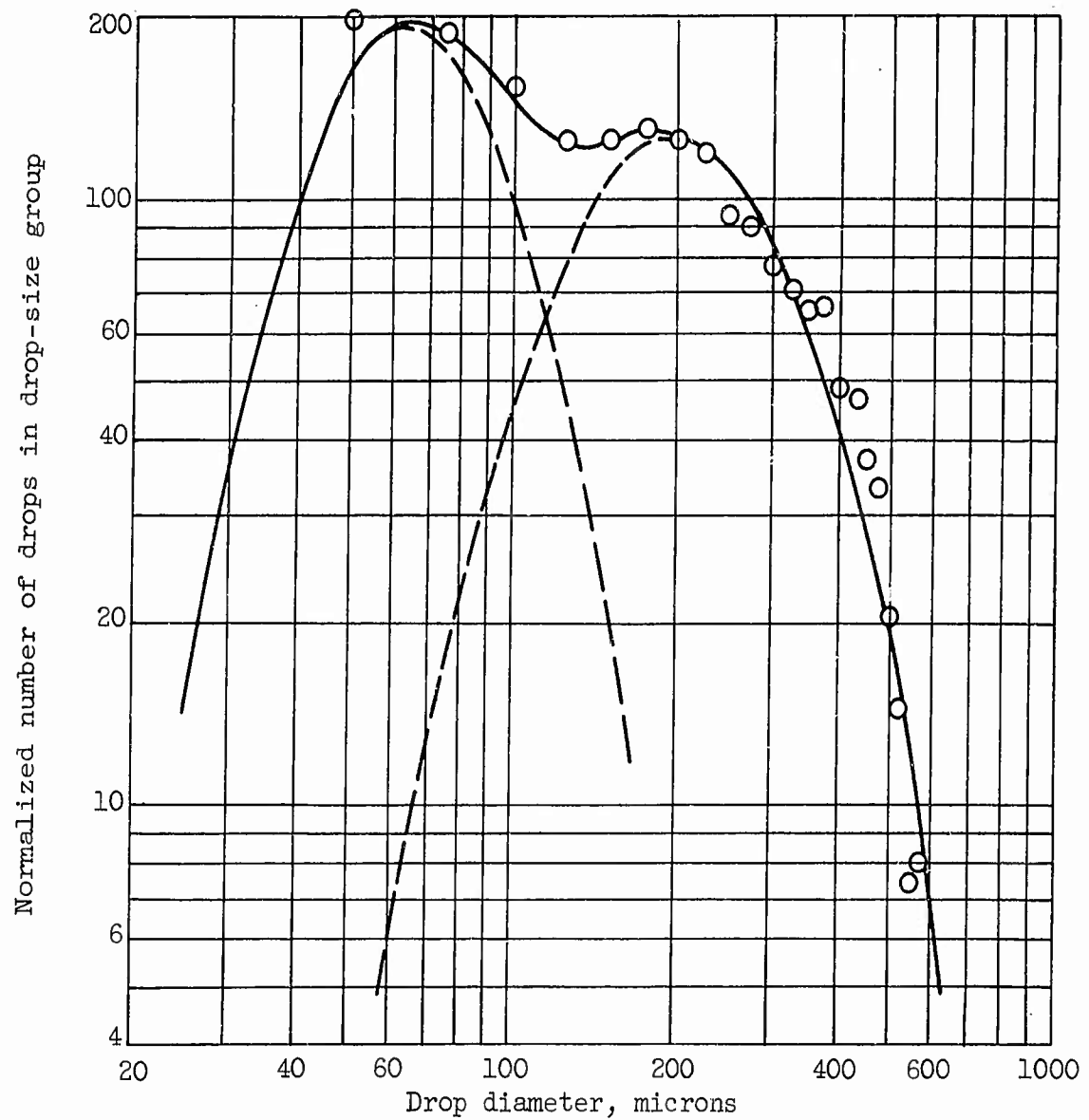


Figure 8. - Number-size distribution from reference study.
Liquid, heptane; jet diameter, 0.06 inch; impingement angle,
 50° ; jet velocity, 65 feet per second; gas velocity, 100 feet
per second; number of drops, 1234.

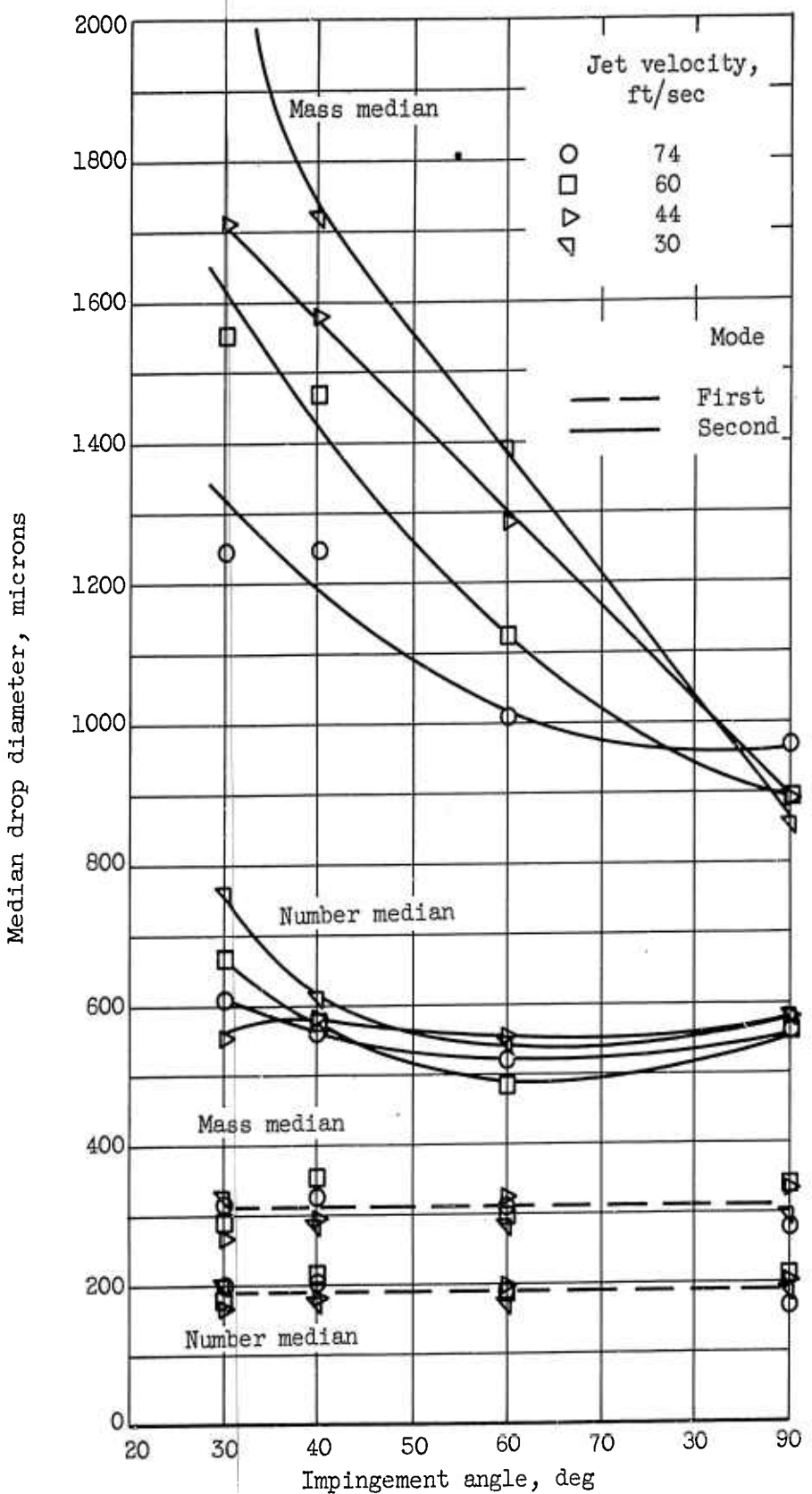


Figure 9. - Effect of impingement angle on median drop sizes in bimodal distribution.

E-1301

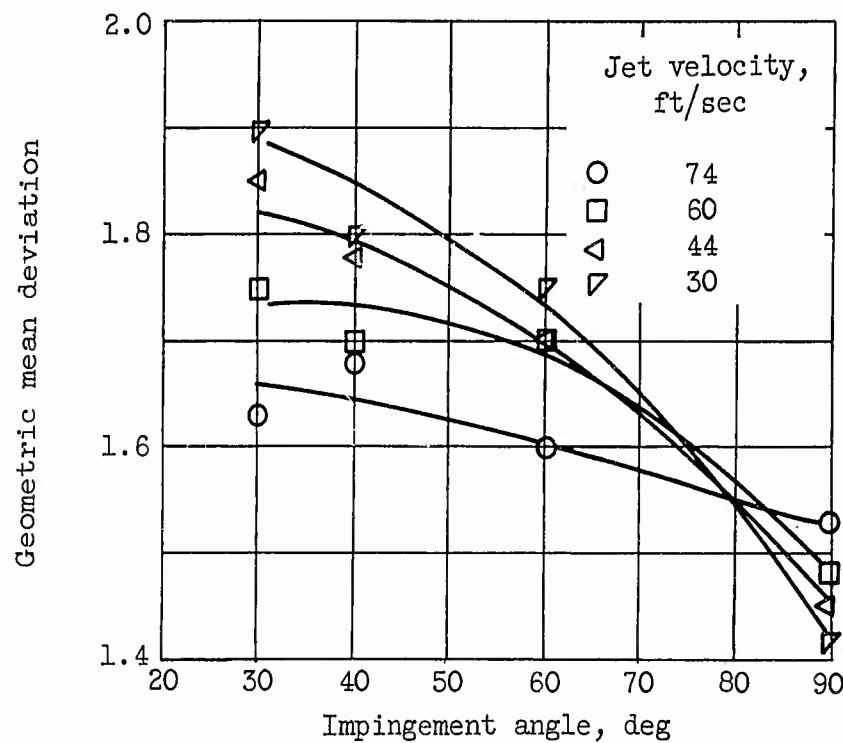


Figure 10. - Effect of impingement angle on geometric mean deviation of second mode.

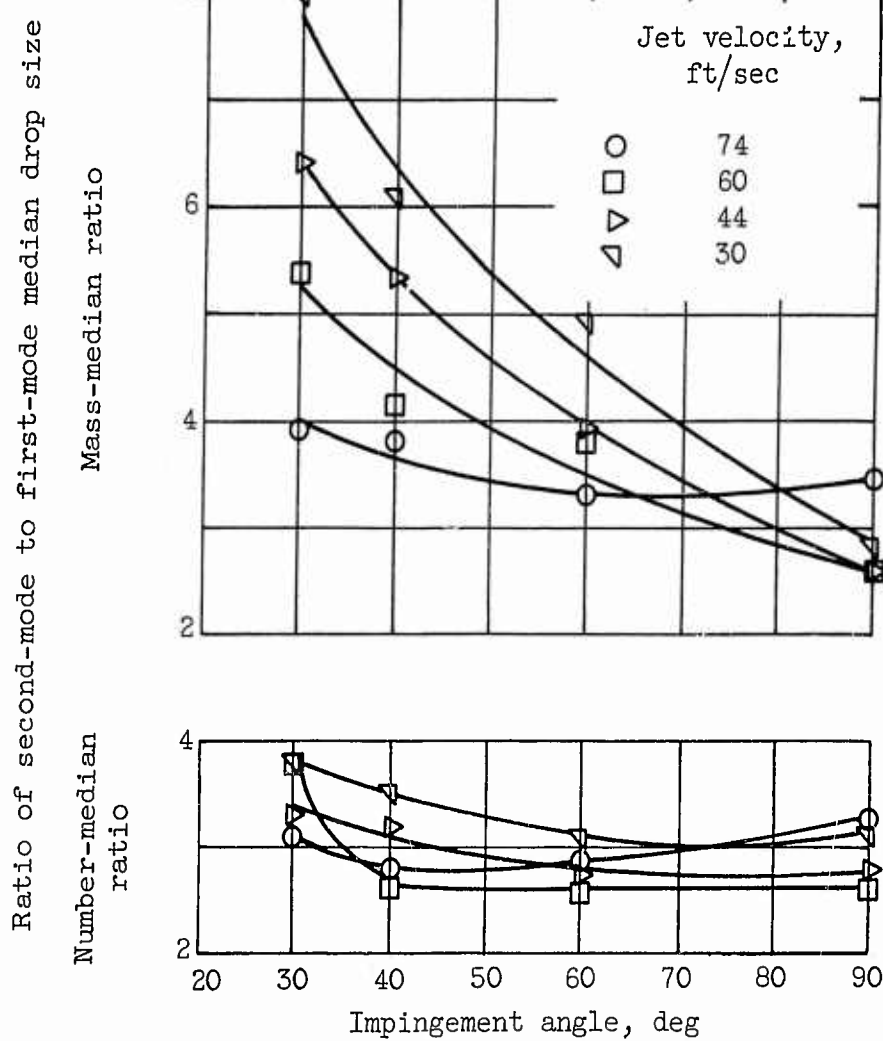


Figure 11. - Effect of impingement angle on ratio of second- to first-mode median drop size.

E-1301

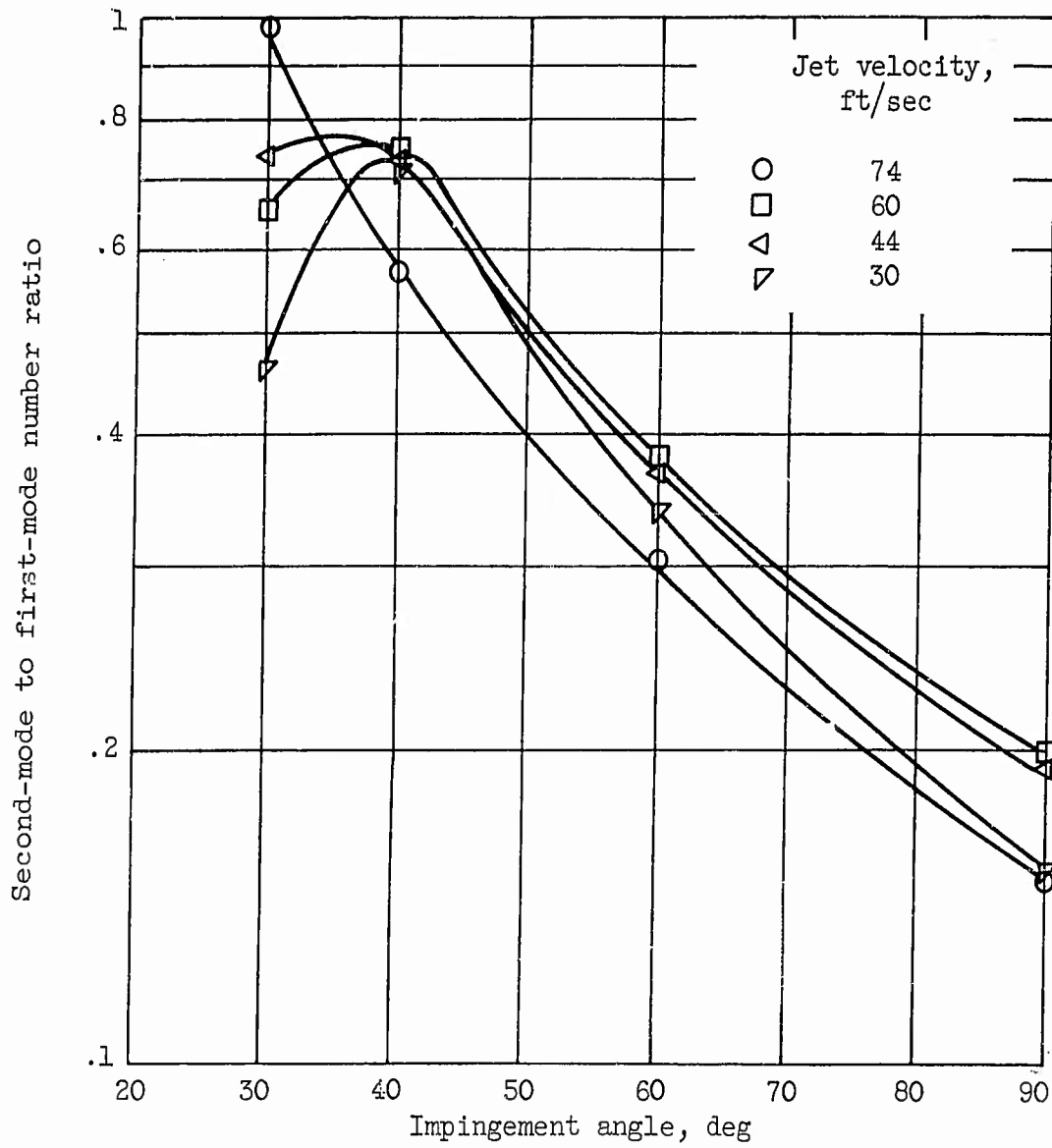


Figure 12. - Effect of impingement angle on ratio of number of drops in bimodal distribution.

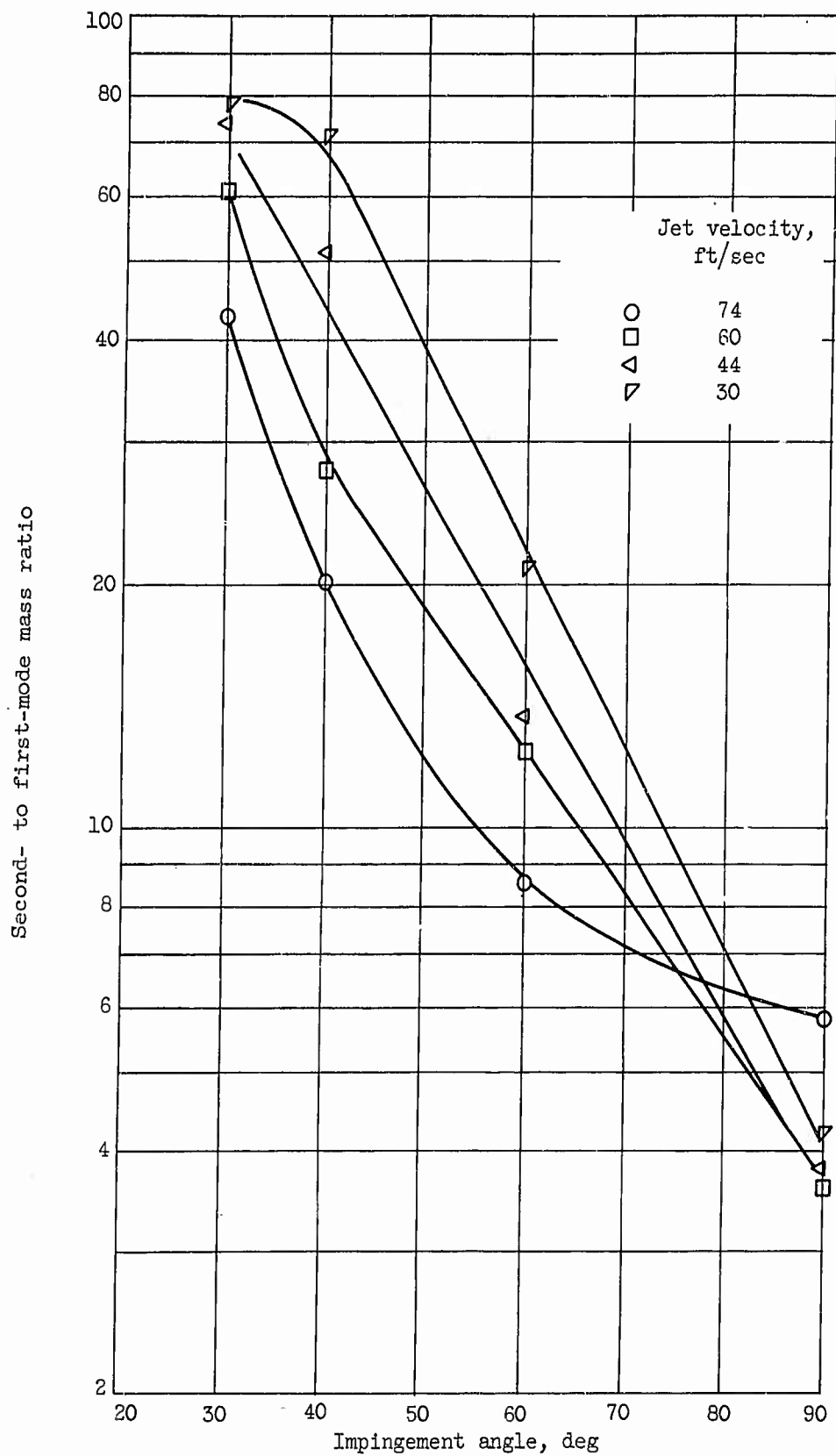


Figure 13. - Effect of impingement angle on ratio of masses in bimodal distribution.

E-1301

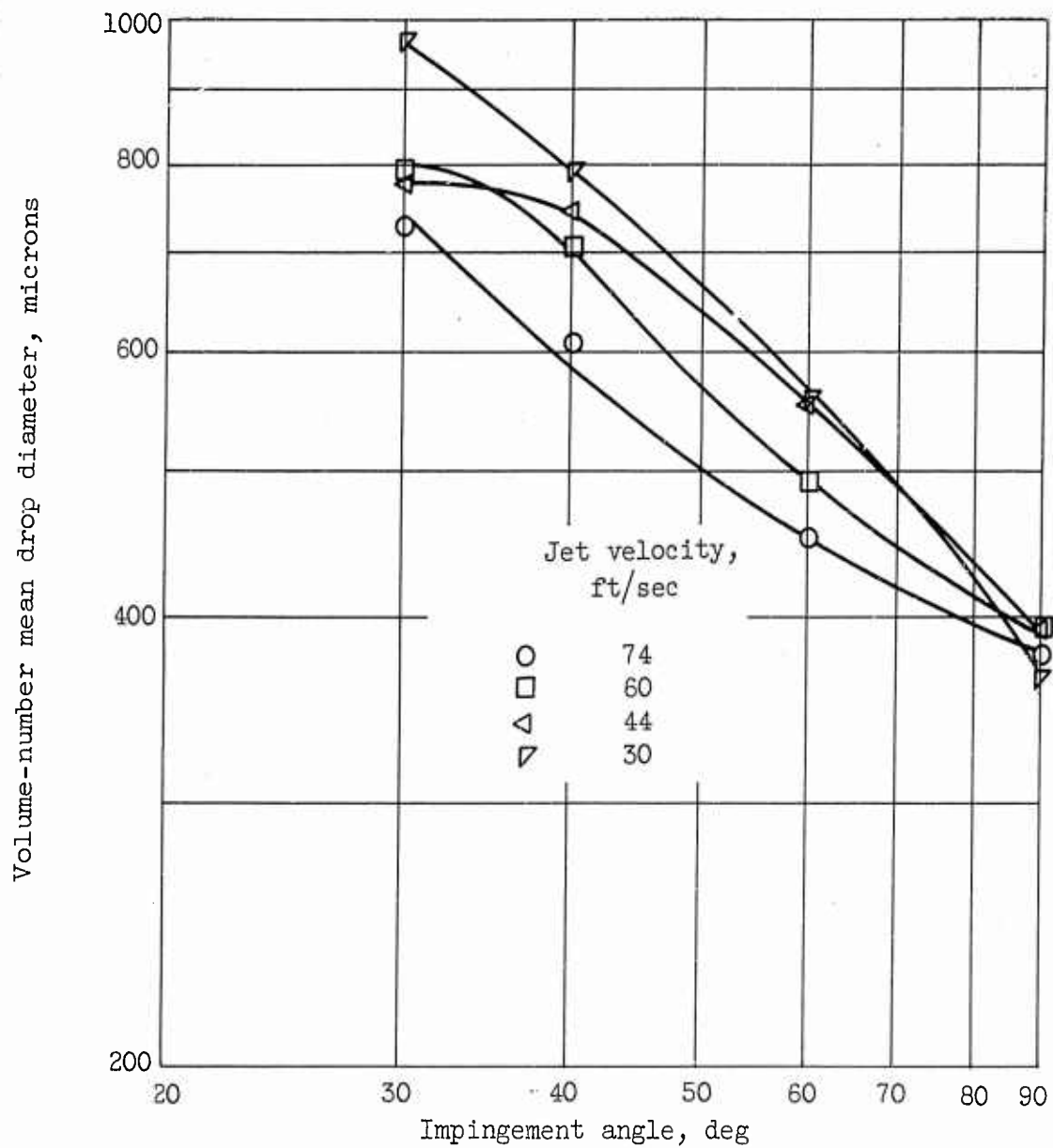


Figure 14. - Effect of impingement angle on volume-number mean drop diameter of spray.

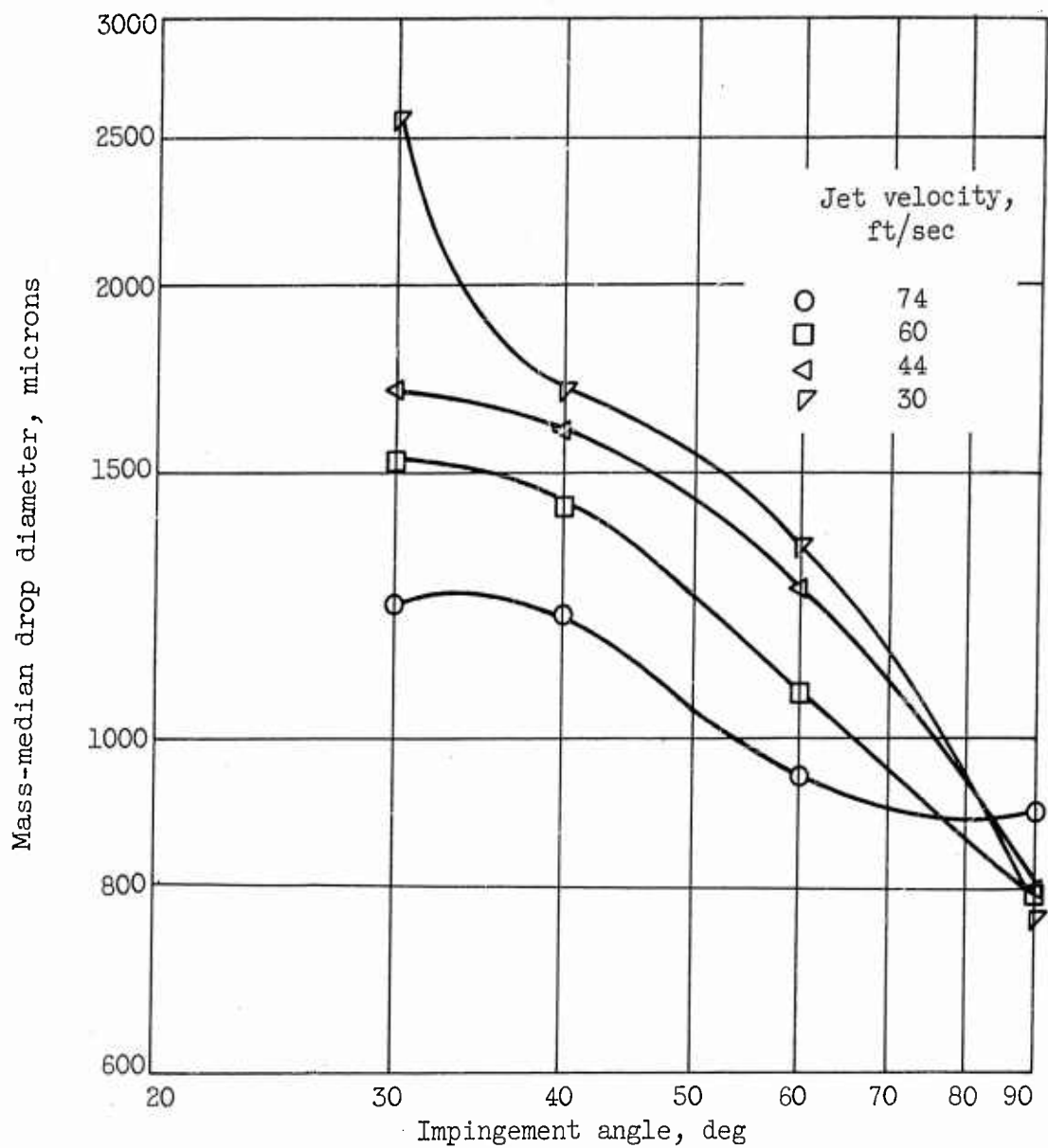


Figure 15. - Effect of impingement angle on mass-median drop diameter of spray.

NASA TN D-872
National Aeronautics and Space Administration.
EFFECT OF IMPINGEMENT ANGLE ON DROP-SIZE
DISTRIBUTION AND SPRAY PATTERN OF TWO
IMPINGING WATER JETS. Marcus F. Heidmann
and Hampton H. Foster. July 1961. 34p. OTS
price, \$1.00. (NASA TECHNICAL NOTE D-872)
Sprays produced by two 0.089-inch-diameter jets at
impingement angles of 10° to 90° and jet velocities
of 30 to 74 feet per second were studied. Drop-size
distributions for sprays formed in 100-foot-per-
second air are presented. Distributions were bimodal
in character, and the effects of test conditions on the
bimodal properties are presented. Photographs of
the over-all spray pattern produced in quiescent air are
also shown.

I. Heidmann, Marcus F.
II. Foster, Hampton Hoge
III. NASA TN D-872
(Initial NASA distribution:
12, Chemical engineering;
20, Fluid mechanics;
37, Propulsion system ele-
ments; 39, Propulsion
systems, liquid-fuel rockets;
44, Propulsion systems,
theory.)

NASA TN D-872

National Aeronautics and Space Administration.
EFFECT OF IMPINGEMENT ANGLE ON DROP-SIZE
DISTRIBUTION AND SPRAY PATTERN OF TWO
IMPINGING WATER JETS. Marcus F. Heidmann
and Hampton H. Foster. July 1961. 34p. OTS
price, \$1.00. (NASA TECHNICAL NOTE D-872)
Sprays produced by two 0.089-inch-diameter jets at
impingement angles of 10° to 90° and jet velocities
of 30 to 74 feet per second were studied. Drop-size
distributions for sprays formed in 100-foot-per-
second air are presented. Distributions were bimodal
in character, and the effects of test conditions on the
bimodal properties are presented. Photographs of
the over-all spray pattern produced in quiescent air are
also shown.

Copies obtainable from NASA, Washington

NASA

Copies obtainable from NASA, Washington

NASA

NASA TN D-872
National Aeronautics and Space Administration.
EFFECT OF IMPINGEMENT ANGLE ON DROP-SIZE
DISTRIBUTION AND SPRAY PATTERN OF TWO
IMPINGING WATER JETS. Marcus F. Heidmann
and Hampton H. Foster. July 1961. 34p. OTS
price, \$1.00. (NASA TECHNICAL NOTE D-872)
Sprays produced by two 0.089-inch-diameter jets at
impingement angles of 10° to 90° and jet velocities
of 30 to 74 feet per second were studied. Drop-size
distributions for sprays formed in 100-foot-per-
second air are presented. Distributions were bimodal
in character, and the effects of test conditions on the
bimodal properties are presented. Photographs of
the over-all spray pattern produced in quiescent air are
also shown.

I. Heidmann, Marcus F.
II. Foster, Hampton Hoge
III. NASA TN D-872
(Initial NASA distribution:
12, Chemical engineering;
20, Fluid mechanics;
37, Propulsion system ele-
ments; 39, Propulsion
systems, liquid-fuel rockets;
44, Propulsion systems,
theory.)

NASA TN D-872

National Aeronautics and Space Administration.
EFFECT OF IMPINGEMENT ANGLE ON DROP-SIZE
DISTRIBUTION AND SPRAY PATTERN OF TWO
IMPINGING WATER JETS. Marcus F. Heidmann
and Hampton H. Foster. July 1961. 34p. OTS
price, \$1.00. (NASA TECHNICAL NOTE D-872)
Sprays produced by two 0.089-inch-diameter jets at
impingement angles of 10° to 90° and jet velocities
of 30 to 74 feet per second were studied. Drop-size
distributions for sprays formed in 100-foot-per-
second air are presented. Distributions were bimodal
in character, and the effects of test conditions on the
bimodal properties are presented. Photographs of
the over-all spray pattern produced in quiescent air are
also shown.

Copies obtainable from NASA, Washington

I. Heidmann, Marcus F.
II. Foster, Hampton Hoge
III. NASA TN D-872
(Initial NASA distribution:
12, Chemical engineering;
20, Fluid mechanics;
37, Propulsion system ele-
ments; 39, Propulsion
systems, liquid-fuel rockets;
44, Propulsion systems,
theory.)

NASA

Copies obtainable from NASA, Washington

NASA

Copies obtainable from NASA, Washington

NASA

<p>NASA TN D-872 National Aeronautics and Space Administration. EFFECT OF IMPINGEMENT ANGLE ON DROP-SIZE DISTRIBUTION AND SPRAY PATTERN OF TWO IMPINGING WATER JETS. Marcus F. Heidmann and Hampton H. Foster. July 1961. 34p. OTS price, \$1.00. (NASA TECHNICAL NOTE D-872)</p> <p>Sprays produced by two 0.089-inch-diameter jets at impingement angles of 10° to 90° and jet velocities of 30 to 74 feet per second were studied. Drop-size distributions for sprays formed in 100-foot-per-second air are presented. Distributions were bimodal in character, and the effects of test conditions on the bimodal properties are presented. Photographs of the over-all spray pattern produced in quiescent air are also shown.</p>	<p>NASA</p>	<p>Copies obtainable from NASA, Washington</p>
<p>NASA TN D-872 National Aeronautics and Space Administration. EFFECT OF IMPINGEMENT ANGLE ON DROP-SIZE DISTRIBUTION AND SPRAY PATTERN OF TWO IMPINGING WATER JETS. Marcus F. Heidmann and Hampton H. Foster. July 1961. 34p. OTS price, \$1.00. (NASA TECHNICAL NOTE D-872)</p> <p>Sprays produced by two 0.089-inch-diameter jets at impingement angles of 10° to 90° and jet velocities of 30 to 74 feet per second were studied. Drop-size distributions for sprays formed in 100-foot-per-second air are presented. Distributions were bimodal in character, and the effects of test conditions on the bimodal properties are presented. Photographs of the over-all spray pattern produced in quiescent air are also shown.</p>	<p>NASA</p>	<p>Copies obtainable from NASA, Washington</p>
<p>I. Heidmann, Marcus F. II. Foster, Hampton Hoge III. NASA TN D-872 (Initial NASA distribution: 12, Chemical engineering; 20, Fluid mechanics; 37, Propulsion system elements; 39, Propulsion systems, liquid-fuel rockets; 44, Propulsion systems, theory.)</p> <p>Sprays produced by two 0.089-inch-diameter jets at impingement angles of 10° to 90° and jet velocities of 30 to 74 feet per second were studied. Drop-size distributions for sprays formed in 100-foot-per-second air are presented. Distributions were bimodal in character, and the effects of test conditions on the bimodal properties are presented. Photographs of the over-all spray pattern produced in quiescent air are also shown.</p>	<p>NASA</p>	<p>Copies obtainable from NASA, Washington</p>
<p>I. Heidmann, Marcus F. II. Foster, Hampton Hoge III. NASA TN D-872 (Initial NASA distribution: 12, Chemical engineering; 20, Fluid mechanics; 37, Propulsion system elements; 39, Propulsion systems, liquid-fuel rockets; 44, Propulsion systems, theory.)</p> <p>Sprays produced by two 0.089-inch-diameter jets at impingement angles of 10° to 90° and jet velocities of 30 to 74 feet per second were studied. Drop-size distributions for sprays formed in 100-foot-per-second air are presented. Distributions were bimodal in character, and the effects of test conditions on the bimodal properties are presented. Photographs of the over-all spray pattern produced in quiescent air are also shown.</p>	<p>NASA</p>	<p>Copies obtainable from NASA, Washington</p>